AD 732032

TRANSPORT PROCESSES IN CERAMIC OXIDES

Order No. 1130, Program Code No. 8D10

Final Technical Report

AVSD-0468-71-RR

15 April 1968 - 15 June 1971

Contract No. DAHC-15-68-C-0296

Expiration Date: 15 June 1971

Project Scientists: T. Vasilos - 617-452-8961
B.J. Wuensch
P.E. Gruber

Contractor: AVCO CORPORATION
Systems Division
Lowell, Massachusetts 01851

DDC
RECEIVED
NOV 9 1971
A

Reproduced by
NATIONAL TECHNICAL
INFORMATION SERVICE
Springfield, Va. 22151

DISTRIBUTION STATEMENT A
Approved for public release;
Distribution Unlimited

80

DISCLAIMER NOTICE

THIS DOCUMENT IS THE BEST QUALITY AVAILABLE.

COPY FURNISHED CONTAINED A SIGNIFICANT NUMBER OF PAGES WHICH DO NOT REPRODUCE LEGIBLY.

UNCLASSIFIED

Security Classification

DOCUMENT CONTROL DATA - R&D

(Security classification of title, body of abstract and indexing annotation must be entered when the overall report is classified)

1 ORIGINATING ACTIVITY (Corporate author)

Avco Corporation, Systems Division, Materials Sciences Department, Lowell Industrial Park, Lowell, Massachusetts 01851

2a REPORT SECURITY CLASSIFICATION: Unclassified

2b GROUP:

3 REPORT TITLE

Transport Processes in Ceramic Oxides

4 DESCRIPTIVE NOTES (Type of report and inclusive dates)

Final Technical Report - 15 April 1968 - 15 June 1971

5 AUTHOR(S) (Last name, first name, initial)

Vasilos, Thomas (Project Scientist)
Wuensch, Bernhardt J.
Gruber, Philip E.

6 REPORT DATE: 15 September 1971

7a TOTAL NO. OF PAGES:

7b NO. OF REFS:

8a CONTRACT OR GRANT NO.: DAHC 15-68-C-0296

b. PROJECT NO. 1130

c. Program Code 8D10

d

9a. ORIGINATOR'S REPORT NUMBER(S)

9b. OTHER REPORT NO(S) (Any other numbers that may be assigned this report)

10 AVAILABILITY/LIMITATION NOTICES

Reproduction in whole or in part is permitted for any purpose of the U.S. Government. Distribution of this document is unlimited.

11 SUPPLEMENTARY NOTES

12. SPONSORING MILITARY ACTIVITY

Materials Research Division
Advanced Research Projects Agency
Washington, D.C.

15. ABSTRACT

Final results are summarized for a program designed to clarify the nature of mass transport in MgO through (1) growth of crystals of improved perfection and purity, (2) measurement of cation self-diffusion rates with the aid of a stable isotope tracer over a wide range of temperatures, and (3) extension of impurity cation and cation self-diffusion measurements to temperatures as close as possible to 2800°C, the melting point of the material.

Crystals of MgO 2 cm in diameter and up to 2 mm in thickness have been grown epitaxially on MgO substrates with the aid of chemical vapor transport with HCl at 1000°C. Growth rates up to 100 micron/hr. have been achieved. Purification results from the process, and negligible concentrations of transport agent are incorporated in the deposit. Cation self-diffusion coefficients have been determined over a temperature range of 1100° - 2400°C, and may be described by D_o of $4.19\ 10^{-4}$ cm^2/sec and an activation energy of 2.76 ± .08 eV. In contrast with previous results, the data appear to represent extrinsic diffusion. The present diffusion coefficients are an order of magnitude smaller than results obtained with the radioisotope Mg^{28} and the discrepancy is attributed to doping resulting from the Si^{28} decay product. Measurements of Ni^{2+} diffusion in MgO have been extended to 2460°C (0.88 T_m). The measurements may be represented by D_o of $1.80\ 10^{-5}$ cm^2/sec and an activation energy of 2.10 eV, a result obtained by previous measurements at much lower temperatures. The present data increase by 70% the temperature range over which data for mass transport are available, but fail to provide evidence for a transition to a region of intrinsic diffusion. No difference in transport behavior is noted for crystals of moderate purity and crystals of the best quality commercially available at present.

DD FORM 1 JAN 64 1473

14 KEY WORDS	LINK A		LINK B		LINK C	
	ROLE	WT	ROLE	WT	ROLE	WT
Diffusion, Mg^{2+} in MgO, Ni^{2+} in MgO Self-Diffusion Impurity diffusion Mass spectrometry Crystal Growth Chemical vapor deposition						

INSTRUCTIONS

1. ORIGINATING ACTIVITY: Enter the name and address of the contractor, subcontractor, grantee, Department of Defense activity or other organization *(corporate author)* issuing the report.

2a. REPORT SECURITY CLASSIFICATION: Enter the overall security classification of the report. Indicate whether "Restricted Data" is included. Marking is to be in accordance with appropriate security regulations.

2b. GROUP: Automatic downgrading is specified in DoD Directive 5200.10 and Armed Forces Industrial Manual. Enter the group number. Also, when applicable, show that optional markings have been used for Group 3 and Group 4 as authorized.

3. REPORT TITLE: Enter the complete report title in all capital letters. Titles in all cases should be unclassified. If a meaningful title cannot be selected without classification, show title classification in all capitals in parenthesis immediately following the title.

4. DESCRIPTIVE NOTES: If appropriate, enter the type of report, e.g., interim, progress, summary, annual, or final. Give the inclusive dates when a specific reporting period is covered.

5. AUTHOR(S): Enter the name(s) of author(s) as shown on or in the report. Enter last name, first name, middle initial. If military, show rank and branch of service. The name of the principal author is an absolute minimum requirement.

6. REPORT DATE: Enter the date of the report as day, month, year; or month, year. If more than one date appears on the report, use date of publication.

7a. TOTAL NUMBER OF PAGES: The total page count should follow normal pagination procedures, i.e., enter the number of pages containing information.

7b. NUMBER OF REFERENCES: Enter the total number of references cited in the report.

8a. CONTRACT OR GRANT NUMBER: If appropriate, enter the applicable number of the contract or grant under which the report was written.

8b, 8c, & 8d. PROJECT NUMBER: Enter the appropriate military department identification, such as project number, subproject number, system numbers, task number, etc.

9a. ORIGINATOR'S REPORT NUMBER(S): Enter the official report number by which the document will be identified and controlled by the originating activity. This number must be unique to this report.

9b. OTHER REPORT NUMBER(S): If the report has been assigned any other report numbers *(either by the originator or by the sponsor)*, also enter this number(s).

10. AVAILABILITY/LIMITATION NOTICES: Enter any limitations on further dissemination of the report, other than those imposed by security classification, using standard statements such as:

(1) "Qualified requesters may obtain copies of this report from DDC."

(2) "Foreign announcement and dissemination of this report by DDC is not authorized."

(3) "U. S. Government agencies may obtain copies of this report directly from DDC. Other qualified DDC users shall request through _____."

(4) "U. S. military agencies may obtain copies of this report directly from DDC. Other qualified users shall request through _____."

(5) "All distribution of this report is controlled. Qualified DDC users shall request through _____."

If the report has been furnished to the Office of Technical Services, Department of Commerce, for sale to the public, indicate this fact and enter the price, if known.

11. SUPPLEMENTARY NOTES: Use for additional explanatory notes.

12. SPONSORING MILITARY ACTIVITY: Enter the name of the departmental project office or laboratory sponsoring *(paying for)* the research and development. Include address.

13. ABSTRACT: Enter an abstract giving a brief and factual summary of the document indicative of the report, even though it may also appear elsewhere in the body of the technical report. If additional space is required, a continuation sheet shall be attached.

It is highly desirable that the abstract of classified reports be unclassified. Each paragraph of the abstract shall end with an indication of the military security classification of the information in the paragraph, represented as *(TS)*, *(S)*, *(C)*, or *(U)*.

There is no limitation on the length of the abstract. However, the suggested length is from 150 to 225 words.

14. KEY WORDS: Key words are technically meaningful terms or short phrases that characterize a report and may be used as index entries for cataloging the report. Key words must be selected so that no security classification is required. Identifiers, such as equipment model designation, trade name, military project code name, geographic location, may be used as key words but will be followed by an indication of technical context. The assignment of links, rules, and weights is optional.

TRANSPORT PROCESSES IN CERAMIC OXIDES

Order No. 1130, Program Code No. 8D10

Final Technical Report

AVSD-0468-71-RR

15 April 1968 - 15 June 1971

Contract No. DAHC-15-68-C-0296

Expiration Date: 15 June 1971

Project Scientists: T. Vasilos - 617-452-8961
B.J. Wuensch
P.E. Gruber

Contractor: AVCO CORPORATION
Systems Division
Lowell, Massachusetts 01851

Details of illustrations in this document may be better studied on microfiche

ABSTRACT

Final results are summarized for a program designed to clarify the nature of mass transport in MgO through (1) growth of crystals of improved perfection and purity, (2) measurement of cation self-diffusion rates with the aid of a stable isotope tracer over a wide range of temperatures, and (3) extension of impurity cation and cation self-diffusion measurements to temperatures as close as possible to 2800°C, the melting point of the material.

Crystals of MgO 2 cm in diameter and up to 2 mm in thickness have been grown epitaxially on MgO substrates with the aid of chemical vapor transport with HCl at 1000°C. Growth rates up to 100 micron/hr. have been achieved. Purification results from the process, and negligible concentrations of transport agent are incorporated in the deposit. Cation self-diffusion coefficients have been determined over a temperature range of 1100° - 2400°C and may be described by D_o of 4.19 10^{-4} cm^2/sec and an activation energy of 2.76 $\pm$ .08 eV. In contrast with previous results, the data appear to represent extrinsic diffusion. The present diffusion coefficients are an order of magnitude smaller than results obtained with the radioisotope Mg^{28} and the discrepancy is attributed to doping resulting from the Si^{28} decay product. Measurements of Ni^{2+} diffusion in MgO have been extended to 2460°C (0.88 T_m). The measurements may be represented by D_o of 1.80 10^{-5} cm^2/sec and an activation energy of 2.10 eV, a result obtained by previous measurements at much lower temperatures. The present data increase by 70% the temperature range over which data for mass transport are available, but fail to provide evidence for a transition to a region of intrinsic diffusion. No difference in transport behavior is noted for crystals of moderate purity and crystals of the best quality commercially available at present.

CONTENTS

I. INTRODUCTION

1.1 Transport Phenomena in Oxides

Many technologically important properties of materials are controlled by mass transport. Ionic electrical conductivity, creep, sintering behavior, and oxidation or solid state reaction rates provide but a few examples of processes in which the migration rates of constituent ions may be the rate-controlling step. An understanding of mass transport rates is therefore essential in any attempt to control or interpret the kinetics of such processes. This has prompted a large number of studies of diffusion in solids. A present, the behavior of simple ionic materials such as the alkali halides is fairly well understood. The role of defect complexes and of impurities in transport mechanisms is known. Reliable estimates, both theoretical and experimental, are available for the energy of formation and migration of point defects. In general, the theoretical and experimental results are in excellent agreement.

Although oxides are a more important class of materials technologically, efforts to extend understanding of mass transport behavior in the alkali halides to oxides have not proven to be straightforward. Theory has been generally unsuccessful in providing energies for defect formation and migration. Experimental work is also more difficult. The high melting points of oxides makes difficult the fabrication of single crystals and the control of their purity. The energy of defect formation in oxides is higher than that of monovalent ionic solids. A smaller concentration of aliovalent impurity may therefore be tolerated if intrinsic transport behavior is to be observed. A few hundred ppm of aliovalent impurities would be sufficient to cause mass transport in most oxides to be dominated by impurities at all temperatures up to their melting points. Few, if any,

/

oxides of the requisite purity have been available until recently. Given a material of marginal purity, one would ordinarily perform transport measurements at temperatures as close as possible to the melting point of the host material in any attempt to reveal intrinsic transport behavior. The high melting point of oxides causes such temperatures to be accessible only with great difficulty. The high vapor pressure of many oxides at elevated temperatures may further complicate such measurements.

A sizable body of data exists for diffusion rates in ceramic oxides. Data are available for both anion and cation transport and, in some cases, a number of impurity cations as well. Such studies have provided data for commercial grade material which has proved useful in the interpretation of kinetics. Usually, however, little insight has been provided into the basic nature of the diffusion process or even whether the transport measured represented intrinsic or impurity-controlled data. The magnitudes of the diffusion parameters which have been observed, and the purity of the materials employed, strongly suggest that impurity controlled data has been measured in most, if not all, studies.

1.2 Status of Transport in Magnesium Oxide

This program is concerned with a single material--magnesium oxide. This material is of considerable technological importance (e.g., as a refractory, in infrared applications, and for utilization as transparent armor). Magnesium oxide has the rock-salt structure possessed by the majority of the alkali halides, and thus might be expected to be an oxide to which understanding of simpler ionic materials might be most readily extended. Further, single crystals, although of questionable purity and perfection, have long been available. Data for anion and cation self-diffusion have

been obtained. Diffusion rates have also been measured for many different impurity cations, (see Table I in Appendix B). With the exception of Ba^{2+} diffusion at low solute penetrations, the diffusion of all impurity cations and O^{2-} is characterized by small values of D_o (ca. 10^{-5} cm^2/sec). The activation energies for diffusion have generally been found to be of the order of 2 eV (1.6 to 2.7 eV). Since MgO has a rock-salt structure, it is expected that the predominant point defect controlling intrinsic transport will be of the Schottky type. Theory has been unable to provide a precise value for the energy of Schottky pair formation, E_f, but one theoretical estimate provides 5 ± 1 eV. The activation energy for intrinsic mass transport in MgO (given by $\frac{1}{2} E_f$ plus the energy for ion migration) would therefore be expected to be 1 or 2 eV in excess of 2.5 eV. Most of the activation energies observed for impurity ion diffusion are of the order of, or less than, $\frac{1}{2} E_f$. This suggests that extrinsic impurity-controlled diffusion has been observed. Such interpretation is supported by the small values of D_o (characteristic of extrinsic transport) which have been observed. Further, if the energy for Schottky pair formation is 5 eV, a few hundred ppm aliovalent impurity would be sufficient to cause transport in MgO to be extrinsic at all temperatures up to 2800°C, the melting point of the material. The majority of the studies which have been performed to date have employed Norton Company MgO. This material typically contains of the order of 1000 ppm cation impurity and would afford little possibility of displaying intrinsic behavior.

The parameters reported for Mg^{2+} self-diffusion stand in marked contrast to the above results. The value of D_o of 10^{-1} cm^2/sec is typical of intrinsic transport. Also, the activation energy of 3.43 eV may be

interpreted as $\frac{1}{2} E_f$ plus a reasonable (ca. 1 eV) energy of ion migration. The cation self-diffusion measurements have therefore been usually interpreted as representing intrinsic transport. This is difficult to reconcile with the bulk of the data available for MgO, since (a) all studies were conducted in a similar temperature range with materials of comparable purity, (b) the Mg^{2+} ion has a radius comparable to that of several of the impurity ions which had been investigated, and (c) the 1 eV energy of motion, while reasonable, is difficult to reconcile with the 1.6 to 2.7 eV activation energy observed for anion and impurity cation migration. Interpretation of the activation energy observed in all of the above studies is hindered by the fact that no results have revealed the change in temperature dependence of the diffusion coefficients which would permit unequivocal identification of the regions of extrinsic or intrinsic transport.

Materials of higher purity had become available in recent years. Intrinsic transport could in principle be observed in such crystals of very high temperatures. To date, however, the high vapor pressure of MgO at elevated temperatures has prevented the measurement of mass transport rate at any temperature higher than two-thirds of the melting point (1850°C).

In the case of the alkali halides, which are ionic conductors, valuable insight into the nature of the transport process has been obtained by combining ionic electrical conductivity measurements with the results of diffusion studies. Such comparison has not proved fruitful for MgO since oxides may conduct charge through either an ionic or electronic mechanism. MgO has been classed as a purely electronic conductor, a purely ionic conductor, and as a mixed conductor by various investigators. The nature of electrical conduction in MgO appears to be a complex function of temperature, oxygen partial pressure, and impurity content. The process will

probably not be understood until careful measurements have been made on crystals of extremely high purity. It is felt that it will be definitive diffusion data which will ultimately assist in the interpretation of conductivity rather than (as in the case of the alkali halides) the conductivity measurements providing insight into the nature of the defect structure.

1.3 Object and Scope of the Present Program

The body of data obtained from mass transport in MgO to date has no unambiguous interpretation and is not self-consistent. Several studies seem desirable to clarify understanding of this material. Most measurements were conducted at a time when available crystals contained 1,000 to 2,000 ppm impurity. Recently, crystals of a nominal 100 ppm impurity content have become commercially available. It should be possible, in principle, to observe intrinsic behavior for this material at very high temperatures. It would be especially significant if a change in transport behavior could be revealed in such crystals at temperatures close to the melting point. Inspection of the results compiled in Table I of Appendix B, however, shows that no measurement of mass transport in MgO had been conducted at a temperature above two-thirds of the melting point of the material. It therefore seemed highly desirable to develop techniques for the preparation of diffusion specimens at still higher temperatures while utilizing crystals of the best quality presently available.

The data for Mg^{2+} self-diffusion form the basis with which all measurements of impurity cation transport must be compared. Previous self-diffusion data have been limited to a narrow range of temperatures because of a lack of a long-lived Mg radioisotope. The longest lived radioisotope is Mg^{28} which has a half-life of only 21.3 hrs. This has restricted previous determinations of cation self-diffusion rates to a narrow range of temperatures (1400-1600°C) for which samples could be prepared in a relatively

short time. Magnesium has three stable isotopes. It would seem possible to employ one of these isotopes as a tracer and thereby eliminate previous time -temperature limitation on experiments.

The main barrier to gaining further insight into diffusion processes in oxides, however, is the lack of single crystals of the requisite purity. It therefore would be extremely desirable to produce single crystals of a purity and perfection superior to those presently available.

The present program was intended to clarify the nature of transport in MgO. In view of the problems described above, the program consisted of four main efforts:

(a) Since experimental study of transport in oxides is limited by the purity of the materials presently available, attempts were to be made to synthesize single crystal MgO of a purity and perfection superior to the crystals presently available. Chemical transport techniques seemed particularly promising in this area and constituted the bulk of this portion of the effort.

(b) Mg^{2+} self-diffusion rates were to be determined over a wider range of temperatures than was heretofore possible. The limitations imposed by lack of a suitable radioisotope were overcome by use of a stable isotope as tracer, and development of mass spectrometer procedures for determining isotopic ratios.

(c) Techniques were to be developed to permit extension of previous studies of impurity ion mass transport and also of cation self-diffusion to much higher temperatures than previously attainable. It was hoped that such measurements

could be extended to a temperature at least of the order of 2500°C (0.9 T_m) to perhaps reveal a region of intrinsic transport.

(d) Realizing that transport measurements are meaningless without adequate characterization of the materials employed, the MgO crystals utilized in the diffusion measurements and also those synthesized in the program were to be characterized as to dislocation density, and impurity time-temperature. Also, it is not clear whether, given material of high perfection and impurity, the necessary sample preparation and annealing techniques may be conducted in such a way as to preserve the quality of the crystals. The mechanical damage and chemical contamination introduced as a result of performing high-temperature transport measurements was therefore to be also ascertained.

II. PROGRAM ACHIEVEMENTS

Substantial success was achieved in each of the main areas of this program. While much additional work could be performed, several portions of the study were brought to completion and have either appeared in press or, alternatively, have been put in the form of essentially completed manuscripts which will shortly be submitted for publication. These reprints or manuscripts are attached in the form of appendices and provide a full technical discussion of details. The following discussion will serve primarily to review the highlights of the accomplishments.

2.1 Crystal Growth

Epitaxial growth of MgO deposits on an MgO single crystal substrate was achieved by HCl transport at 1000°C. Growth rates of 100 microns per

hour were obtained, and crystals up to several mm in thickness and 2 cm in diameter have been synthesized. The growth rates achieved are comparable to those encountered in flux growth methods. The dislocation densities of the deposits were superior in general to those of the substrates. It was demonstrated that considerable purification occurred as a result of the transport process. While the bulk of the effort was directed at establishment of growth kinetics, crystals grown from high-purity starting powder had impurity approaching that of the best single crystals commercially available.

2.2 High Temperature Mass Transport Measurements

Techniques were perfected to permit annealing of samples at very high temperatures where the vapor pressure of both the diffusion solute and the host crystal were extremely high. The basis of the technique consists of encapsulation of the diffusion specimen in a pressed cylinder of high purity MgO powder. This procedure provides several advantages. The surface of the host crystal, which would ordinarily vaporize at a rate several orders of magnitude greater than the diffusion rate, was protected from vaporization. The encapsulation also entrapped the small amounts of solute present in thin film varieties of diffusion specimens. In the case of NiO diffusion in MgO, for example, samples were successfully prepared at temperatures nearly 400°C above the melting point of pure solute. The technique further protected the sample from contamination by impurities derived from furnace elements, as well as fixing the composition of the atmosphere with which the sample was in equilibrium.

Samples were successfully prepared at temperatures up to 2460°C (0.9 T_m). This represents an extension by 70% of the temperature range over

which mass transport data for MgO were previously available.

2.3 Stable Isotope Analysis

Techniques were successfully developed for analysis through mass spectrometry of the very small (5×10^{-4} gm) amounts of sample removed in the course of diffusion couple sectioning. These techniques should be applicable to the study of diffusion of other stable isotopes as well. The procedure has several inherent advantages. First and primarily, the problem of use of a difficult or expensive radioisotope is avoided. Secondly, since an isotopic ratio is determined, the technique is not affected by accidental loss of a portion of the material removed in sectioning. The primary inconvenience of the method is that it was relatively time consuming. The mass spectrometer had to be baked out and evacuated upon introduction of each of the 10 to 20 sections removed from a given diffusion sample. Furthermore, in the study of magnesium self-diffusion, a high natural abundance of the stable isotope tracer occurred in the sample. The concentration gradient was thus obtained as the difference of two relatively large numbers and was accordingly subject to inaccuracies which were large compared to those encountered in the more usual measurement of the activity of sections containing a radioisotope.

2.4 Impurity-Cation Diffusion at High Temperatures

Measurements of Ni^{2+} diffusion in both high and moderate purity MgO single crystals were extended to a temperature of 2460°C. Surprisingly, it was found that the two grades of crystals employed displayed essentially the same transport behavior despite notably different dislocation densities and impurity contents. The results could be adequately described in terms of an extrapolation of data obtained at lower temperatures (1000-1850°C) obtained in an earlier study in this laboratory. The best crystals

commercially available are thus still not of a quality sufficient to display intrinsic diffusion even at 9/10 of the melting temperature. It is intriguing to note, however, that at the highest temperatures which were successfully achieved, the measured diffusion coefficients appeared to deviate increasingly from the Arrhenius plot. This deviation was larger (a factor of 3) than could be explained in terms of experimental error. It thus appears that a transition to a new transport mechanism may be commencing at temperatures in excess of 2400°C. This observation must, however, be made with some reservation since samples are extraordinarily difficult to prepare at these temperatures.

2.5 Effects of Transmutation Products on Transport Rates

Using the stable isotope, Mg^{26}, cation self-diffusion measurements were determined in single crystal MgO over a temperature range of 1100° - 2400°C. The present results are an order of magnitude smaller than data previously obtained with the short-lived radioisotope Mg^{28} over a much narrower temperature range (1400-1600°C). The present results could be described in terms of a pre-exponential term D_o of 4.19×10^{-4} cm^2/sec and an activation energy of $2.76 \pm .08$ eV. The present results clear up the apparent inconsistency between the previous results reported for cation self-diffusion and the body of data obtained for divalent impurity cation diffusion; the value of D_o and activation energy for cation self-diffusion obtained in the present work are comparable to the parameters found for impurity ion migration. This, plus the fact that the present diffusion coefficients are smaller than those which had previously been assumed to represent intrinsic diffusion, appears to indicate that cation self-diffusion in magnesium oxide is also extrinsic in nature. The order-of-magnitude difference of the diffusion coefficients encountered in the present work

raises, however, an interesting and fundamental question in connection with the use of radioisotopes to determine self-diffusion rates in ionic materials. If the isotope has an extremely short half-life and, further, if the isotope transmutes into a cation of different valence, it is possible that the decay products dope the crystal to an extent that intrinsic transport behavior might never be observable in a host crystal of any initial purity as a result of introduction of the products of radioactive decay.

2.6 Future Plans

Much significant work remains to be done in each of the areas explored in the present program. In the area of crystal growth, primary emphasis was on optimization of kinetics to achieve useful and reproducible growth rates. While purification of the source MgO was demonstrated, utilization of high purity starting material was only partially explored. It was shown that the chemical purity of the deposit depends in large extent on the purity of the source material. Another interesting prospect not yet examined would be the use of multiple transport stages to enhance the purity of the deposits still further.

Cation self-diffusion measurements were made in both moderate and high purity single crystals. The bulk of the measurements, however, were made with the material of moderate impurity, although it is the highest purity crystals which are of greatest interest. The less pure material was used in initial measurements while perfecting analytical techniques. The rate at which the mass spectrometer analyses could be performed determined the rate at which data could be obtained. Consequently, many more diffusion specimens were actually prepared than could be analyzed under the present program. In particular, at each of the temperatures for which a diffusion coefficient in moderate purity material is reported, a duplicate sample was

prepared with high purity crystals. The decision to concentrate on the moderate grade material was, in a sense, a pragmatic one. It became apparent toward termination of this program that all analyses could not be completed. Since a considerable body of data had been obtained for the moderate purity crystals, it seemed desirable to obtain as complete a set of measurements for one material rather than scattered data for two different grades of crystals. This course was followed, and seemed justified in view of the fact that no significant difference in behavior was noted between the two grades of crystals. Nevertheless, a complete series of high purity diffusion specimens have in fact been prepared. It is hoped that these samples will eventually be analyzed under some future program.

The attached appendices contain manuscripts describing growth of MgO crystals by chemical vapor deposition techniques, the diffusion of nickel in high purity MgO at high temperatures, and cation self-diffusion measurements in MgO. These manuscripts are in essentially final form. One of the objectives of the ARPA mass transport program, however, was to generate interlaboratory cooperation. This was indeed stimulated in the present program. While the effort at Avco has been concluded, several studies of relevance to the present results are underway in other laboratories. Samples of some of the materials mass-analyzed in the present program, as well as some samples which we believe to be of the highest purity yet produced in this program, have been provided to the U.S. National Bureau of Standards for analysis. These analyses will provide, it is hoped, confirmation of the analyses described in this report and also demonstrate that crystals of purity superior to those presently described have, in fact, been actually synthesized. With their permission, it is hoped that these results will eventually be incorporated into the paper on crystal growth. Similarly, a

program under Professor A.H. Heuer at Case Western Reserve University has been concerned with the use of activation analysis in the measurement of extremely shallow concentration gradients. It appears as though these techniques might be applicable to the study of the diffusion of Mg^{26} in MgO. Accordingly, samples have been prepared at temperatures still lower than those described in Appendix B and provided to Professor Heuer. These samples were prepared in a temperature range in which diffusion coefficients were so small that production of gradients of an extent suitable for sectioning would have required prohibitively long diffusion annealings. If the activation analyses are successful, data extending the range of the present measurements by 100 or 200°C will be available. It is hoped that these data will eventually be incorporated in the manuscript concerning cation self-diffusion.

III. PRESENTATIONS AND PUBLICATIONS

The results of the present study have or will be described in the following presentations and publications.

1. B.J. Wuensch and T. Vasilos, "Mass Transport in MgO at High Temperatures," Paper 37-b-71, presented before the 73rd Annual Meeting of the American Ceramic Society, Chicago, April 28, 1971 (Abstract in Bull. Am. Ceram. Soc., 50, (4), 373 (1971).
2. B.J. Wuensch and T. Vasilos, "Diffusion of Ni^{2+} in High Purity MgO at High Temperatures," J. Chem. Phys., 54 (3), 1123-1129 (1971) (Appendix A).
3. B.J. Wuensch, W.C. Steele, and T. Vasilos, "Cation Self-Diffusion in Single Crystal MgO," (to be submitted to J. Chem. Phys.) (Appendix B).
4. P.E. Gruber, "Growth of High Purity MgO Single Crystal by Chemical Vapor Transport Techniques" (to be submitted to J. Cryst. Growth) (Appendix C).

APPENDIX A

Diffusion of Ni^{2+} in High Purity MgO at High Temperatures

Reprinted from

The Journal of Chemical Physics
54 (3), 1123-1129 (1971)

Reprinted from:

THE JOURNAL OF CHEMICAL PHYSICS VOLUME 54, NUMBER 3 1 FEBRUARY 1971

Diffusion of Ni^{2+} in High-Purity MgO at High Temperatures

B. J. WUENSCH AND T. VASILOS

AVCO Corporation, Systems Division, Lowell, Massachusetts 01851

(Received 2 September 1970)

Electron microbeam probe spectroscopy has been used to determine diffusion coefficients for Ni^{2+} in moderate- and high-purity MgO single crystals in an argon atmosphere over a temperature range of 1900–2460°C. Samples were encapsulated in pressed cylinders of MgO powder for protection against contamination and volatilization of both solute and host crystal. No study of mass transport in MgO had previously been extended to temperatures greater than 0.66 T_M. The present measurements extend to 0.88 T_M but fail to reveal a change in transport mechanism. An activation energy of 2.10 eV and D_0 of 1.80×10^{-5} cm²/sec, previously obtained from measurements between 1000 and 1850°C, adequately describe the present results. No significant difference in transport rates was noted between the two grades of crystals employed despite notably different dislocation densities and impurity contents.

INTRODUCTION

Magnesium oxide would appear to be an oxide to which understanding of transport in simpler materials such as the alkali halides, might be readily extended. MgO has the rocksalt structure, and single crystals have long been available. For these reasons diffusion rates for a number of ions in this oxide have been determined. Data are available for both cation[1] and anion[2] self-diffusion rates, and also for a number of impurity cations[3]: Ni^{2+}, Co^{2+}, Fe^{2+}, Mn^{2+}, Zn^{2+}, Be^{2+}, Ca^{2+}, and Ba^{2+}.

Interpretation of these results has not proved to be straightforward. No study has revealed the change in the temperature dependence of the diffusion coefficient which would permit unambiguous identification of regimes of intrinsic and extrinsic mass transport. Theory has, in general, been unsuccessful in providing an accurate estimate of the energy required for Schottky pair formation in MgO. One calculation[4] provides 5±1 eV. If this value is accepted, the activation energy for intrinsic mass transport (given by one-half the energy of defect formation plus the energy of motion) should be 1 or 2 eV in excess of 2.5 eV. However, the activation energy for O^{2-} self-diffusion and the activation energies for impurity cation diffusion have been found to be in the range 1.6–2.7 eV. These values, along with small pre-exponential terms D_0 (typically 10^{-5} cm²/sec), strongly suggest that extrinsic diffusion has been measured. The purity of the crystals employed in most studies supports this conclusion. The 5 eV estimate for Schottky pair formation indicates that a few hundred parts-per-million aliovalent impurity would be sufficient to cause mass transport in MgO to be extrinsic at all temperatures up to the melting point of the material (2800°C). Most data have been obtained with crystals containing of the order of 1000 ppm cation impurity for which intrinsic behavior would be highly unlikely.

The data for Mg^{2+} self-diffusion (and also Ba^{2+})[5] are in marked contrast with other results. The activation energies of 3.4 eV and D_0 of 10^{-1} cm²/sec which have been reported seem to indicate a different diffusion mechanism and are reasonable values for an intrinsic process. The 1 eV energy of motion implied by this interpretation, however, is difficult to reconcile with the data available for impurity ion migration. Further, the Mg^{2+} ion has essentially the same radius as several of the transition metal ions, and it is therefore difficult to understand why cation self-diffusion should behave so differently.

Two investigations therefore seemed desirable to clarify the nature of mass transport in MgO. The measurements of cation self-diffusion[1]—thus far restricted to a narrow range of temperatures (1400–1600°C) for lack of a long-lived radioisotope—should be extended over a wider temperature range to confirm the unusually high activation energy for diffusion.[6] Second, transport measurements with MgO crystals of the best quality available should be extended to temperatures as close as possible to the melting point of MgO. The latter measurements would normally be undertaken in any attempt to reveal a range of intrinsic transport in a material of marginal purity. Unfortunately, the high melting point of MgO causes such temperatures to be accessible only with difficulty. The extremely high vapor pressure of MgO at elevated temperatures further complicates such experiments. No measurement of mass transport in MgO has consequently been conducted at a temperature above 1850°C ($0.66T_M$).

The present study has been concerned with extending earlier measurements[7] of Ni^{2+} diffusion to as high a temperature as possible. Measurements have been successfully completed to $0.88T_M$. Crystals of the highest purity presently available have been employed as well as crystals of moderate purity typical of those studied in earlier work.

THEORY

Two types of boundary conditions were employed in the preparation of specimens. In a first type, a thin film of solute was placed between two slabs of host material. Provided that the diffusion coefficient D is independent of concentration, an annealing

16

TABLE I. Spark-source mass spectrometer analysis of typical MgO crystals after utilization in diffusion couples (parts-per-million weight).

Element	Spicer MgO	Norton MgO	Element	Spicer MgO	Norton MgO
Li	0.05	0.5	Fe	70	200
Na	6	20	Co	0.4	1
Al	20	20	Ni[a]	100	100
Si	10	3	Cu	20	60
S	50	300	Zn	<2	6
Cl	7	20	As	2	4
K	6	10	Sb	6	20
Ca	25	50	W[b]	30	150
Ti	5	50	Σ Cation	213	501
Cr	40	7	Σ Anion	57	320
Mn	3	50	Total	270	821

[a] Remnant of diffusion couple solute.

[b] Derived from furnace elements.

produces a Gaussian distribution of solute which is given by

$$C(x,t) = S(4\pi Dt)^{-1/2} \exp[-x^2(4Dt)^{-1}], \quad (1)$$

where C is solute concentration, S is the initial concentration of solute per unit area, x is distance from the coated interface, and t is the duration of the diffusion annealing. A plot of the logarithm of concentration as a function of the square of solute penetration should therefore be linear with slope equal to $-(4Dt)^{-1}$.

In a second type of specimen, a surface of the host crystal was exposed to a vapor of the solute during annealing. The surface was thus maintained at constant concentration during the course of the experiment. For these conditions

$$C(x,t) = C_0 \operatorname{erfc}[x(4Dt)^{-1/2}], \quad (2)$$

where C_0 is the surface concentration, and erfc represents the complementary Gaussian error function. A plot of $\operatorname{erfc}^{-1}(C/C_0)$ should vary linearly with penetration, and have slope equal to $(4Dt)^{-1/2}$.

EXPERIMENTAL

Materials. Two types of MgO single crystals were employed. Crystals quoted as 4 N purity were obtained from W. & C. Spicer, Ltd., Cheltenham, England. This material probably represents the purest MgO crystals presently available.[8] At the quoted purity it would, in principle, be possible to observe intrinsic transport at very high temperatures. Crystals obtained from the Norton Company, Worcester, Massachusetts have been employed in many previous studies, and were investigated in the present work for purposes of comparison. This material is of variable purity. Typical analyses indicate the presence of 1000 ppm cation impurity.

The purity of crystals of these materials was examined with spark source mass spectrometry. The analyses were performed *after* the crystals had been utilized as diffusion specimens so that any contamination acquired as a result of the high temperature diffusion annealing would be included. Table I lists the elements detectable (at minimum sensitivity of 1 ppm). The Ni present in the analyses represents remnants of solute. The W probably represents contamination derived from furnace elements. Excluding these two elements, the total (anion plus cation) impurity content of the crystals is 270 and 821 ppm weight for the Spicer and Norton materials, respectively.

The dislocation content of the two materials was estimated from etch-pit measurements. Both types of crystals contained subgrains 600–1200 μ in diam. Dislocation densities were in the range $0.7–1.0\times10^5$ cm^{-2} and $1.1–2.5\times10^5$ cm^{-2} for the Spicer and Norton materials, respectively. When the contribution of dislocations at subgrain boundaries was excluded, corresponding densities were $2.8–6.7\times10^4$ and $5.0–16\times10^4$ cm^{-2}.

Solute was, in all cases, applied to a cleaved (100) surface of the host crystal. Such surfaces were optically

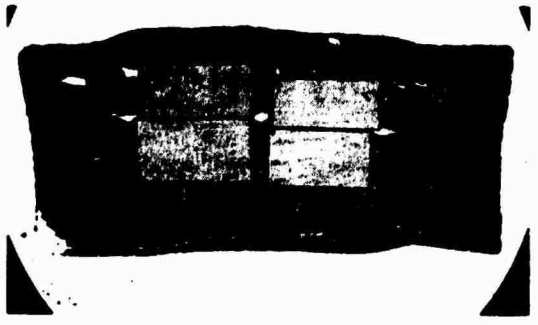

FIG. 1. Section through MgO cylinder encapsulating two thin film diffusion specimens annealed 17.5 h at 1900°C. Crystal size 4 mm. Bright inclusions are pores containing remnants of the conductive coating applied for microprobe analysis.

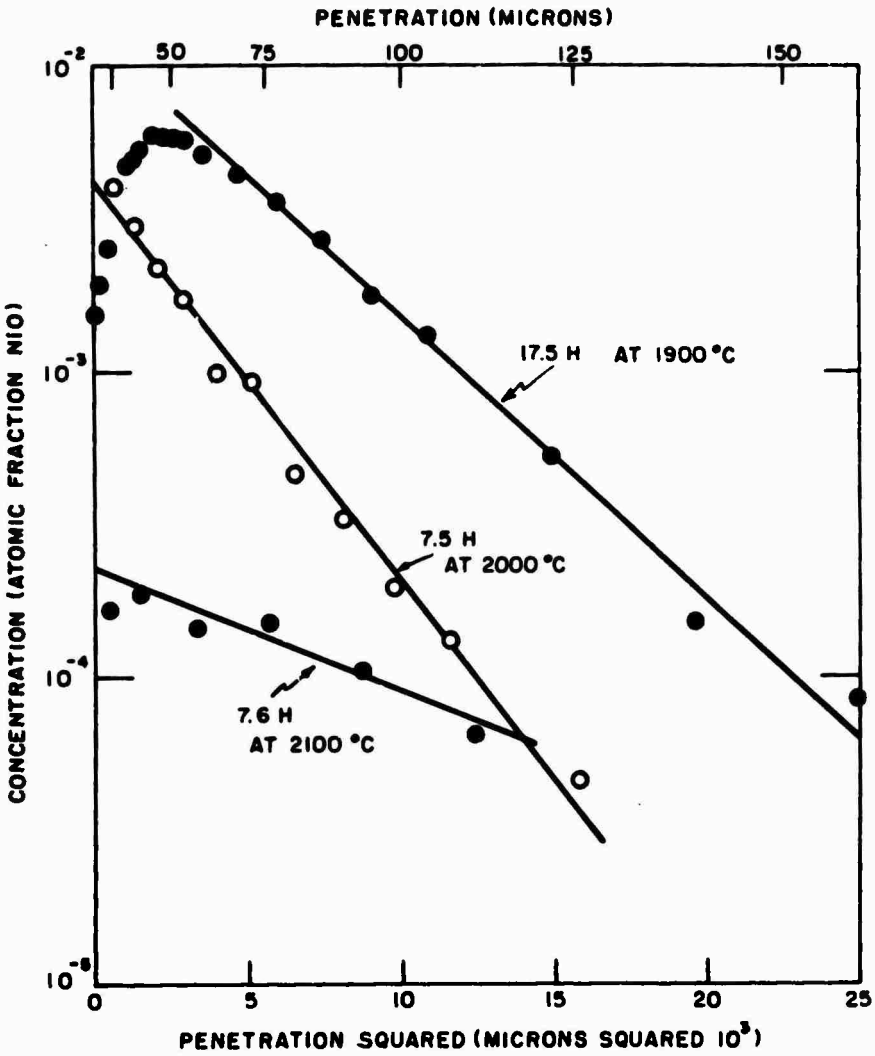

FIG. 2. The logarithm of solute concentration as a function of the square of penetration for representative thin-film specimens of Norton MgO.

flat over short range distances, but displayed 0.5–1-μ cleavage steps. Mechanical damage in the form of excess dislocations along intersecting (110) slip bands was visible near steps. The damage was found to extend a few tens of microns into the crystal. Enhanced transport along boundaries in MgO occurs only in the presence of impurity segregation[9] and, further, all concentration gradients extended 5 to 8 times the depth of the cleavage damage. The effect was therefore not a cause of concern and was considered preferable to the additional damage and contamination which might have been attendant upon further treatment of the crystal surface.

Sample Preparation. Two effects caused severe difficulty in the preparation of diffusion specimens. At the elevated temperatures which were employed (1900–2500°C), MgO had an extremely high vapor pressure, while that of the NiO solute was even higher. (The highest temperature at which a sample was successfully prepared was 370°C above the melting point of NiO.) It was therefore necessary to protect the specimen from vaporization, from possible contamination derived from furnace elements, and to prevent depletion of the source of Ni^{2+} solute. This was accomplished by encapsulating the entire diffusion specimen within a pressed cylinder of high purity MgO powder. The compact sintered during the early stages of the diffusion annealing and thus entrapped the solute. Considerable care was necessary in fabrication of the protective compact to prevent the capsule from spalling as it shrunk about the dense single crystal core. If the capsule cracked, all solute was rapidly lost through vaporization.

Thin film specimens were prepared by depositing a layer of nickel chloride from solution onto a cleaved (100) surface of a host crystal. The chloride was then

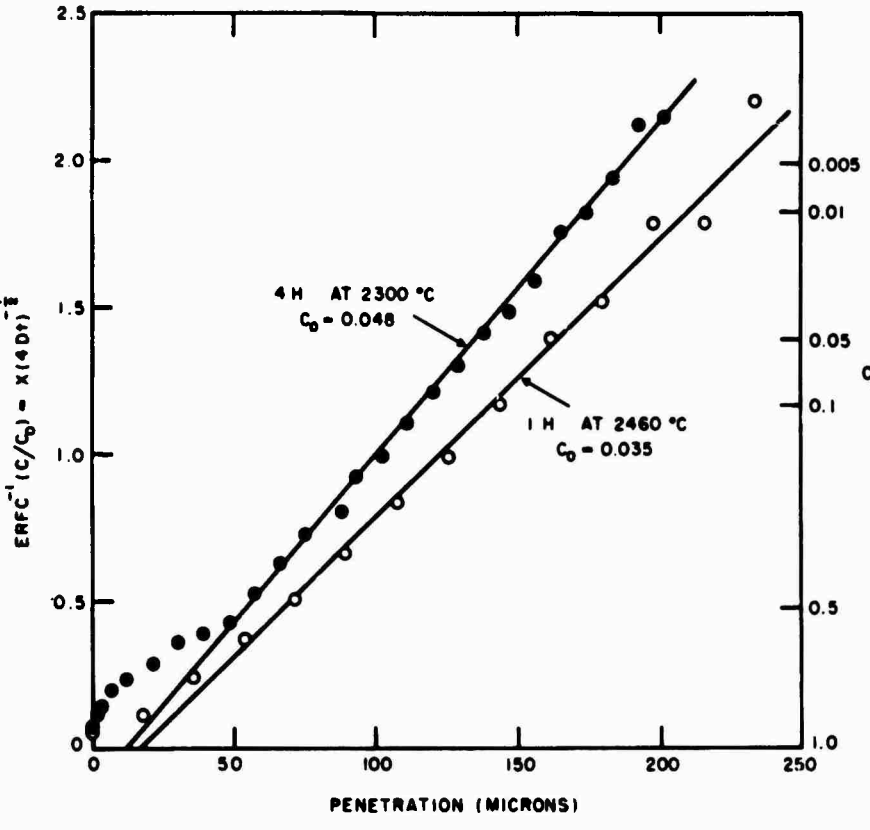

FIG. 3. Plot of $erfc^{-1}$ (C/C_0) as a function of solute penetration for representative vapor-exchange specimens of Norton MgO. (C_0 is surface concentration expressed as atomic fraction NiO.)

converted to a film of NiO a fraction of a micron in thickness by heating in air. The surface of a second crystal was placed over the coated surface. The assembly was then encapsulated. No problem in crystal–solute contact was encountered because of the high vapor pressure of NiO. This type of specimen was successfully employed at temperatures up to the melting point of NiO (2090°C).

A vapor-exchange technique was employed at higher temperatures. A small well was ground in a single crystal of the same material from which the diffusion sample was to be prepared. The well was partially filled with NiO. A prepared (100) surface of a MgO host crystal was placed over the well, and the assembly was then encapsulated. The surface of the host crystal was thus exposed to a vapor of the solute and maintained at constant concentration during the course of the annealing. The high vapor pressure of the MgO particles at the highest temperatures employed did not permit densification of the compact. The capsule did, however, maintain the integrity of the sample long enough to permit the host crystal to bond to the single crystal well and thereby trap the solute. The vapor-exchange technique provided two advantages. The total amount of solute was greater and thus proportionately larger losses of solute could be tolerated. Secondly, the host crystal was never in contact with pure solute which, at temperatures above 2090°C, would have been in a liquid state.

All diffusion annealings were conducted in an argon atmosphere in a controlled tantalum resistance furnace. Temperature was measured pyrometrically. Vapor-exchange specimens were successfully prepared at temperatures up to 2460°C ($0.88T_M$). Above this temperature two-thirds of the NiO–MgO solid solution series was above the solidus of the system and difficulty with melting at the sample surface was encountered.

Sample Analysis. The capsules were cut upon completion of the diffusion annealing to expose a surface normal to the solute-coated interface. An exposed surface of a capsule enclosing two thin film specimens is illustrated in Fig. 1. Concentration gradients in the host crystal were determined with the aid of electron microbeam probe spectroscopy. It proved necessary to coat the exposed surface of the specimens with a thin film of carbon to render the sample conductive and prevent charge buildup during analysis. Samples were analyzed with a 30 kV electron beam having a nominal 1-μ diameter. Ni$K\alpha$ fluorescent intensities were recorded relative to the intensity obtained from a sample of pure Ni to eliminate possible effects of beam fluctuations. Recorded intensity

TABLE II. Diffusion coefficients for Ni^{2+} in single crystal MgO.

Temp. (°C)	Time (h)	Specimen type[a]	Diffusion coefficient (cm^2/sec) Norton MgO	Spicer MgO	Extrapolation of low temperature data[b]
1900	17.5	T	1.37×10^{-10} 2.40×10^{-10}	2.29×10^{-10} 2.64×10^{-10}	2.47×10^{-10}
2000[c]	7.5	T	2.12×10^{-10} 3.08×10^{-10}	4.99×10^{-10} 5.41×10^{-10}	4.05×10^{-10}
2100	7.6	T	9.86×10^{-10}	1.65×10^{-9}	6.36×10^{-10}
2200	5.0	V	1.35×10^{-9}	7.34×10^{-10}	9.61×10^{-10}
2300	4.0	V	1.39×10^{-9}	...	1.42×10^{-9}
2300	4.0	V	1.96×10^{-9}	1.44×10^{-9}	1.42×10^{-9}
2400	3.0	V	3.38×10^{-9}	2.40×10^{-9}	2.01×10^{-9}
2460	1.0	V	6.59×10^{-9} 7.77×10^{-9}	8.49×10^{-9}	2.45×10^{-9}

[a] T = thin film specimen, V = vapor-exchange specimen.
[b] Reference 7.
[c] Crystals used for analyses of Table I.

ratios were converted to concentration with the aid of a calibration curve obtained from a set of fine-grained NiO–MgO standards.

RESULTS

Typical concentration gradients obtained for the thin film type of specimen are presented in Fig. 2 where, according to (1), the logarithm of concentration is plotted as a function of the square of penetration. The gradient presented for 1900°C was selected to illustrate an anomaly which was encountered in a few specimens. Loss of solute toward the completion of the diffusion annealing caused the Ni^{2+} to rediffuse out of the specimen. This produced a drop in concentration near the surface of the sample. It was assumed that this effect had no influence on portions of the gradient well into the interior of the specimen. The gradients obtained at 2100°C were produced just above the melting point of pure NiO. Solute loss was severe and the retained NiO concentrations were extremely small. This sample provided the least accurate diffusion coefficient obtained in the study.

Figure 3 presents plots of $\text{erfc}^{-1}(C/C_0)$ as a function of solute penetration which are typical of those obtained for vapor-exchange specimens. The slight perturbation in concentration near the surface in one gradient again represents loss of solute in the final stages of the diffusion annealing. It may be noted that neither curve in Fig. 3 extrapolates to zero at zero penetration. The shift in apparent surface position is due in large part to the NiO incorporated in the crystal. The integrated NiO content of the gradient, when converted to an equivalent layer of pure NiO, provides a surface displacement which is in fair agreement with the intercept. The displacement of the surface in all cases represented only 5% to 6% of the total extent of the gradient. The effect of the moving boundary was therefore assumed to be negligible.

A total of 20 diffusion coefficients were measured at temperatures between 1900 and 2460°C. The results are summarized in Table II. Braces enclose values obtained from different crystals which had been annealed together in the same run. Separate entries for a given temperature indicate results from different crystals employed in separate experiments. Each diffusion coefficient represents an average of values obtained from microprobe scans performed at different locations along the solute-coated interface. Agreement ranged from 6% to 21% depending upon the quality of the gradient. The average reproducibility of all measurements was 12%. Table II also presents the diffusion coefficient predicted by extrapolation of earlier measurements[7] made in air at lower temperatures (1000–1850°C). The diffusion coefficients determined in the present study are in close agreement with the extrapolated values.

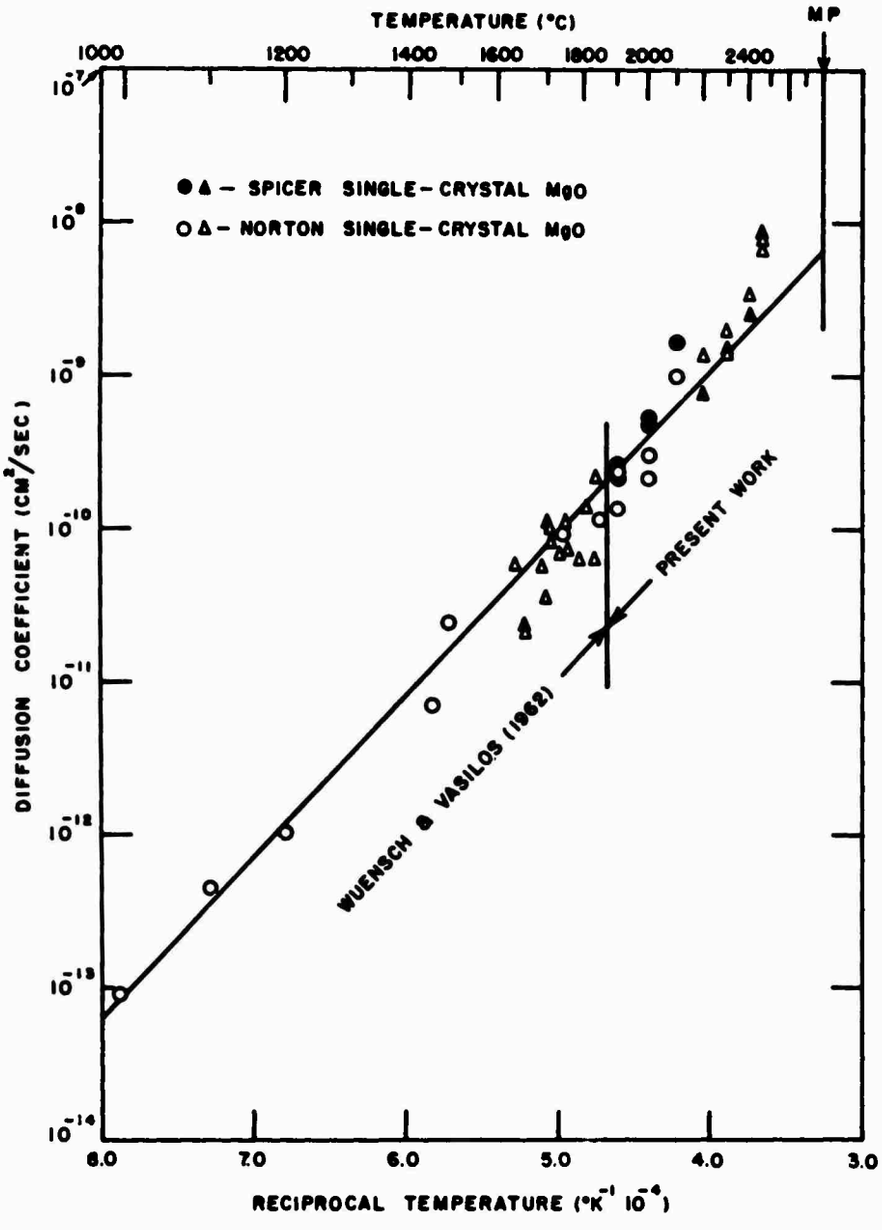

FIG. 4. Diffusion coefficients for Ni^{2+} in single crystal MgO as a function of reciprocal temperature. (Triangles represent data obtained from vapor-exchange specimens; circles thin-film samples.)

Figure 4 gives the present diffusion coefficients plus data previously obtained[7] plotted as a function of reciprocal temperature. The line used to describe the results is given by

$$D = 1.80(10)^{-5} \exp(-2.10\,\text{eV}/kT)$$

and is the same as had been used to describe the low temperature results.

DISCUSSION

The present measurements increase by 70% the temperature range for which mass transport has been measured in MgO. Despite the fact that the upper limit of observation has been increased from 0.66 to 0.88 of the melting point of the material, no change in transport mechanism is apparent. Extrapolation of data obtained at lower temperatures adequately

describes the present results. Since it appears probable that the transport observed represents an extrinsic process, one must conclude that the best MgO crystals presently available are not yet of sufficient quality to display intrinsic behavior. It is rather surprising that the Spicer material, while notably superior in perfection and purity, does not display a behavior which is significantly different from that of the Norton crystals. Several interpretations are possible. The defect structure of MgO may be dominated by impurities other than cations: OH^- is known to be a major impurity in MgO. While not measured in the present work, both sorts of crystals could have comparable hydroxyl content since they are prepared through similar processes. An alternative possibility is that Ni^{2+} when diffusing in MgO creates vacancies through a certain fraction of the solute existing in the trivalent state. A consequence of this, however, would be a concentration-dependent diffusion coefficient. The data of the present study could be interpreted within experimental error by (1) and (2), which assume D to be independent of concentration. It is worth noting, however, that other measurements of Ni^{2+} diffusion in MgO (which employed semi-infinite source boundary conditions) *have* revealed a concentration-dependent diffusion coefficient[10] (in air, but not in vacuum). No study employing thin film or vapor-exchange boundary conditions has revealed this dependence. No real explanation can be given for this discrepancy, but it should be noted that (a) very different ranges of solute concentrations have been explored in the two types of experiments (10^{-4} to 10^{-2} for the thin film and vapor-exchange experiments versus 0.1 to 0.5 for the semi-infinite source), and (b) the high concentration portion of the gradient in the present types of specimens is confined to regions near the surface where a concentration dependence might be masked by the perturbations noted above.

It is of interest to note that, at the highest temperatures of the present work, the observed diffusion coefficients appear to increasingly deviate from the extrapolation of the low temperature data. At the highest temperature achieved, the measured values are larger by a factor of 3. This discrepancy seems too large to be explained by experimental uncertainty. This result must be interpreted with extreme caution because samples are extraordinarily difficult to prepare at these temperatures. Uncertainty exists as to the effective time and temperature of the annealing because of the short time for which the specimen may be maintained at temperature. The main significance of the highest datum is that it exists at all! Nevertheless, it appears as though a change to a new transport mechanism may be commencing at temperatures above 2400°C. It would be of great interest to extend measurements to slightly higher temperatures to confirm this trend. This was not possible in the system NiO–MgO because of the difficulty experienced with melting of the sample. However, the study of cation self-diffusion which is in progress will not be subject to this limitation.

ACKNOWLEDGMENTS

The writers are pleased to acknowledge the assistance of A. Moschetti in the preparation of samples. W. H. Rhodes performed the microstructure characterizations. The spark-source mass spectrometer analyses were performed by D. C. Walters of the Battelle Memorial Institute. The study was supported by the Advanced Research Projects Agency under Contract DAHC15-68-C-0296.

[1] R. Lindner and G. D. Parfitt, J. Chem. Phys. 26, 182 (1957).
[2] Y. Oishi and W. D. Kingery, J. Chem. Phys. 33, 905 (1960).
[3] Recent data have been summarized by B. J. Wuensch and T. Vasilos, Natl. Bur. Std. (U.S.), Spec. Publ. 296, 95 (1968).
[4] J. Yamashita and T. Kurosawa, J. Phys. Soc. Japan 9, 944 (1954).
[5] B. C. Harding, Phil. Mag. 16, 1039 (1967).
[6] Measurements employing a stable isotope of Mg are in progress and will be reported at a later date. Our preliminary results confirm a high activation energy (2.92 eV), but smaller than previously reported.
[7] B. J. Wuensch and T. Vasilos, J. Chem. Phys. 36, 2917 (1962).
[8] J. W. Cleland, Natl. Bur. Std. (U.S.), Spec. Publ. 296, 195 (1968).
[9] B. J. Wuensch and T. Vasilos, J. Am. Ceram. Soc. 49, 433 (1966).
[10] S. L. Blank and J. A. Pask, J. Am. Ceram. Soc. 52, 669 (1969).

APPENDIX B

Cation Self-Diffusion in Single Crystal MgO

(Submitted to the Journal of Chemical Physics)

Cation Self-Diffusion in Single-Crystal MgO

B.J. Wuensch, W.C. Steele and T. Vasilos

Avco Corporation, Systems Division, Lowell, Massachusetts 01851

Cation self-diffusion coefficients have been obtained for MgO in an argon atmosphere over a temperature range of 1100° to 2400°C from concentration gradients determined with the aid of mass spectrometry. The problems associated with use of the short-lived radioisotope Mg^{28} were avoided by employing the stable isotope Mg^{26} as a tracer. Samples were prepared utilizing vapor-exchange, thick-film, and semi-infinite source boundary conditions at high, intermediate and low temperatures, respectively, and were protected from contamination and volatilization by encapsulation in cylinders of pressed MgO powder. No significant difference in transport behavior was noted between crystals of moderate quality and those of the highest purity presently available. The temperature dependence of the diffusion coefficients may be represented by an activation energy of 2.76 $\pm$ .08 eV and D_o of 4.19 10^{-4} cm^2/sec. These parameters are comparable to those

previously reported for impurity ion diffusion. The activation energy obtained is interpreted as that for cation migration. Previous measurements of cation self-diffusion coefficients obtained with the short-lived radioisotope Mg^{28} are an order of magnitude larger and have been interpreted as intrinsic diffusion. The discrepency is attributed to doping introduced by the Si^{28} decay product of Mg^{28}.

INTRODUCTION

Mass transport in the alkali halides is fairly well understood. Theoretical and experimental measures of the energies for defect formation, migration and association are available and, in general, are in close accord. Extension of this understanding to oxides has not been straightforward. Magnesium oxide has been extensively investigated, partly because it is a material of considerable technological importance, but mainly because it has the rock salt crystal structure and would appear to be an oxide to which understanding of the alkali halides might be readily extended. Furthermore, single crystals, although of questionable character, have long been available. Data have therefore been obtained for both anion[1] and cation[2] self-diffusion, and for a large number of divalent and trivalent impurity cations.[3-11] Table I summarizes the results obtained in tracer-type experiments. Not included in the compilation are the results of studies of interdiffusion between two oxides. Measurements of the latter sort have been performed for MgO-NiO[12-15], CoO[12], FeO[14,16], MnO[17], Fe_2O_3[14], Cr_2O_3[18], Al_2O_3[19], and $MgAl_2O_4$[20].

None of the above studies has revealed a change in the temperature dependence of the diffusion coefficients which were measured. It is therefore difficult to identify any given set of data as representing either intrinsic or extrinsic (impurity controlled) mass transport, and to deduce energies for defect formation and migration. Indirect evidence, however, strongly suggests that extrinsic behavior has been observed in most, if not all, studies. While theory has been unable to provide a precise value of the energy for Schottky defect pair formation in MgO, one such estimate[22] provides $E_f = 5 \pm 1$ eV, while an empirical correlation of defect formation energies with melting temperatures[23] predicts $E_f = 6.6$ eV, and $E_m = 2.6$ eV.

If such is the case, a few hundred ppm of aliovalent impurity would be sufficient to cause mass transport in MgO to be impurity-controlled at all temperatures up to its melting point (2800°C). Most of the measurements of Table I were performed with crystals containing of the order of 1000 ppm cation impurity for which there would be little possibility of observing intrinsic diffusion. The parameters summarized in Table I support this conclusion. The small values of D_o, typically 10^{-5} cm^2/sec, are indicative of extrinsic transport. Similarly, an activation energy for intrinsic diffusion should be given by $\frac{1}{2} E_f + E_m$ where E_m is the energy for ion migration. Most of the energies of Table I are less than, or of the order of, half of the available estimates for E_f.

The data for Mg^{2+} self-diffusion[2] (and also Ba^{2+} diffusion at low solute penetrations[11]) stand in marked contrast to other results. The magnitudes of $D_o(10^{-1}$ $cm^2/sec)$ are reasonable values for an intrinsic process, and the activation energies may be interpreted as $\frac{1}{2} E_f$ plus a reasonable energy (ca. 1 eV) for ion migration. This interpretation, however, is difficult to reconcile with the bulk of the transport data obtained for MgO. The 1 eV energy of motion is much smaller than the energies of migration found for impurity cation and O^{2-} diffusion. The cation self-diffusion data were obtained over a similar temperature range and with crystals from the same source as in many of the impurity ion measurements. Mg^{2+} has a radius similar to that of several of the impurity cations which have been studied, and it is therefore difficult to understand why cation self-diffusion should behave differently.

Magnesium oxide crystals of improved quality have become available in recent years[24]. At the purities which have been reported, it should be possible, in principal, to observe intrinsic transport at very high temperatures. Such measurements, however, are extremely difficult to perform

because of the high vapor pressure of MgO at elevated temperatures. As a result, as inspection of Table I shows, no measurements (with the exception of one recent study[7]) have been conducted at a temperature above 1850°C. This represents only 0.69 T_m in °K. Measurement of the important cation self-diffusion data has been further hampered by the lack of a convenient radioisotope. The longest-lived radioisotope, Mg^{28}, has a half-life of only 21.3 h.

The present study reports measurement of cation self-diffusion rates in single-crystal MgO at temperatures as close to the melting point of the material as possible. Data were successfully obtained over a temperature range of 1100° to 2400°C (0.45 to 0.87 T_m in °K). The problems associated with use of a short-lived radioisotope were circumvented through use of a stable isotope, Mg^{26} (natural abundance 11.17%), as tracer.

Increased attention is presently being given to the preparation of oxide crystals of high purity and perfection, since lack of suitable materials remains the principal obstacle to improved understanding of mass transport in oxides. It is not obvious, however, whether such perfection may be preserved throughout the treatment necessary for the preparation of samples in property measurements at very high temperatures. Considerable discussion is therefore devoted to the characterization of crystals and to the sample preparation techniques which were employed.

THEORY

Boundary conditions Because of the wide range of temperatures explored, a number of different boundary conditions were employed in the preparation of samples. An exposed surface of a host single-crystal was equilibrated with a vapor of isotope during the diffusion annealing conducted at the highest temperatures. A surface of the specimen was thereby maintained at constant concentration during the experiment. After a time, t, under these conditions

$$X(x,t) = X_S \text{ erfc } \left[x(4Dt)^{-\frac{1}{2}} \right] \qquad (1)$$

where X is the concentration of isotope diffused into the specimen at a distance x from the surface, X_S is surface concentration, and erfc is the complementary Gaussian error function. A plot of the inverse complementary error function of X/X_S should, therefore, vary linearly with penetration. A value of the diffusion coefficient, D, may be obtained from

$$d \left[\text{erfc}^{-1} (X/X_S) \right] / d\, x = (4Dt)^{-\frac{1}{2}} \qquad (2)$$

At lower temperatures ($< 1600^{\circ}C$) the surface concentration of tracer isotope was not sufficiently in excess of the natural abundance to permit use of this type of specimen. The isotope was instead applied in the form of an initial coating. A typical radioisotope experiment utilizes an initial solute coating which is very thin in comparison with the extent of the final gradient. Under such conditions, an annealing of duration t produces a Gaussian distribution of solute

$$X(x,t) = S(4\pi Dt)^{-\frac{1}{2}} \exp \left[-x^2(4Dt)^{-1} \right] \qquad (3)$$

where S is the initial concentration of solute per unit area. This set of boundary conditions was not applicable in the present study because of the

unusual situation created by the presence of a high "background" natural abundance of tracer (11.17%). The concentration distribution given by (3) decreases with time. It would not have been possible to produce tracer penetrations of an extent suitable for subsequent analysis through mechanical section and yet maintain concentration at a sufficiently high level above "background". The only parameter which may be adjusted to meet both requirements is S, the initial concentration of solute per unit area. This, in turn, may be accomplished only through coating of the host crystal with an isotopic layer of thickness h which is <u>not</u> negligible relative to the extent of the diffusion zone. The solute distribution is then given by a less familiar solution to the diffusion equation[25]:

$$X(x,t) = \tfrac{1}{2}X_s \left[\text{erf } (h-x)(4Dt)^{-\frac{1}{2}} + \text{erf } (h+x)(4Dt)^{-\frac{1}{2}} \right] \qquad (4)$$

where erf is the Gaussian error function, and X_s is the uniform concentration of solute in the initial layer. This solution unfortunately cannot be cast in a form in which a simple function of X would vary linearly with some function of solute penetration to yield a slope related to D. If h is known, however, (by direct measurement, or by integration of the solute contained in the gradient) an estimate of $(4Dt)^{-\frac{1}{2}}$ may be obtained from the surface concentration:

$$(4Dt)^{-\frac{1}{2}} = 1/h \text{ erf}^{-1} \left[X(x=0)/X_s \right] \qquad (5)$$

or, alternatively (without knowledge of h) by application of (3) as an approximation to the concentration distribution measured at highest penetrations. The initial estimate of $(4Dt)^{-\frac{1}{2}}$ may be refined with the entire experimental gradient by iteration with the exact solution (4).

It proved necessary to employ the "thick film" samples over only a narrow range of intermediate temperatures. At still lower temperatures, the extent of the gradient was so slight that a layer of isotope thick in

comparison could be deposited on the crystal. (Such specimens could have also been prepared in the temperature range for which the "thick film" solution was utilized, but sectioning through the very thick deposit which would have been required would have been extremely time consuming.) Semi-infinite source boundary conditions apply in this circumstance and

$$X(x,t) = \tfrac{1}{2} X_s \operatorname{erfc}\left[x(4Dt)^{-1}\right] \tag{6}$$

where x is now distance from the solute-host crystal interface. A value of D may be obtained from

$$d\left[\operatorname{erfc}^{-1}(2X/X_s)\right]/dx = (4Dt)^{-1} \tag{7}$$

application of which does not require knowledge of h. The behavior of (4) is such that (6) is approximately valid when $(h^2/Dt)^{\frac{1}{2}} > 4$.

Relation Between Solute Concentration and Isotope Ratio

The high natural abundance of stable tracer isotope in the host crystal introduced a subtle point in connection with specification of solute concentration from a measured isotopic ratio. The initial isotopic composition of the MgO host crystal was

$$C_0^{24} + C_0^{25} + C_0^{26} = 1 \tag{8}$$

where C_0 is the natural abundance of the stable isotopic oxides ^{24}MgO, ^{25}MgO and ^{26}MgO (atomic fractions of 0.7870, 0.1013, and 0.1117, respectively). A concentration of tracer isotope X^{26} diffused into the crystal substitutes for all three species and

$$X^{26} + (1 - X^{26})(C_0^{24} + C_0^{25} + C_0^{26}) = 1 \tag{9}$$

The <u>total</u> concentration of ^{26}MgO is thus

$$C^{26} = X^{26} + (1 - X^{26})\ C_0^{26} \tag{10}$$

In terms of an experimentally measured ratio of a pair of isotopes (e.g. $R_{26/24}$), from (9),

$$X^{26} = (C_0^{24} R_{26/24} - C_0^{26}) \left[C_0^{24} R_{26/24} + (1 - C_0^{26}) \right]^{-1}, \qquad (11)$$

and

$$C^{26} = C_0^{24} R_{26/24} \left[C_0^{24} R_{26/24} + (1 - C_0^{26}) \right]^{-1} \qquad (12)$$

The amount of diffused tracer, X^{26}, is <u>not</u> equal to $C^{26} - C_0^{26}$, the total concentration of isotopic oxide less its natural abundance. The two quantities are actually related by

$$X^{26} = (1 - C_0^{26})^{-1} \ (C^{26} - C_0^{26}) \qquad (13)$$

The two measures of solute concentration differ, however, only by a constant factor $(1 - C_0^{26}) = 0.8883$. This factor cancels in (2) and (7) and is of no importance in (3) and (4). The experimentally measured solute distributions may thus be equally well described in terms of either X^{26} or $C^{26} - C_0^{26}$. We have chosen the latter quantity since it provides a more direct appreciation of a level of concentration relative to the "background" natural abundance.

EXPERIMENTAL

Materials Two types of MgO single crystals were employed. The majority of the measurements were performed with crystals obtained from the Norton Company, Worcester, Massachusetts. This material has been employed in the majority of previous studies of mass transport in MgO, but is only of moderate purity. Crystals quoted as 4N purity were obtained from W. & C. Spicer, Ltd., Cheltenham, England. This material probably represents the purest MgO crystals commercially available at present[24] and, in principal, should be capable of displaying intrinsic transport behavior at very high temperatures. A previous study of Ni^{2+} diffusion in MgO, however, failed to reveal any significant difference in the transport properties of the Norton and Spicer materials[7].

Spark source mass spectrometry was used to determine the purity of the two different materials. The analyses were performed after utilization of the crystals as diffusion specimens so that any contamination acquired as a result of sample preparation and the subsequent diffusion annealing would be included in the result. Table II lists the elements detectable (at minimum sensitivity of 1 ppm). The total impurity contents (264 and 700 ppm wt for the Spicer and Norton materials, respectively) are similar to the results of analyses previously reported[7].

Dislocation contents were estimated for a number of crystals of both types through counting of the pits produced after etching for 15 min. at room temperature in a solution consisting of 1 part concentrated H_2SO_4, 1 part distilled water and 5 parts, by volume, of saturated ammonium chloride solution. Both types of crystals were found to contain subgrains 600 to 1200 μ in diameter, Figure 1c. Dislocation densities were in the

range 0.7 to 1.0 10^5 cm^{-2} and 1.1 to 2.5 10^5 cm^{-2} for Spicer and Norton MgO, respectively. Upon exclusion of the contribution of dislocations at subgrains, the corresponding densities become 2.8 to 6.7 10^4 and 5.0 to 16 10^4 cm^{-2}, respectively.

The isotope employed was obtained from the Oak Ridge National Laboratory as a fine-grained MgO powder enriched to 98.78% $Mg^{26}O$. The material unfortunately contained nearly 0.2% impurity (Si 0.07, Pt 0.05, Ca and Cu 0.01, and Fe 0.03) as determined in a spectrographic analysis performed at Oak Ridge. These impurity levels were of considerable concern, particularly in subsequent preparation of thick-film and semi-infinite-source specimens.

Crystal Preparation The solute isotope was applied to a (100) surface of the host crystal. Cleaved surfaces, while flat over short-range distances, were found to display 0.5 to 1 μ cleavage steps. Extensive mechanical damage in the form of excess dislocations along intersecting (110) slip bands was observed near such steps, Fig. 1a. This damage was found to extend approximately 40 μ into the surface. The mechanical damage was considered undesirable and, further, the surface roughness was unacceptable for those samples to be annealed at low temperatures for which the concentration gradients were anticipated to be shallow. Mechanical polishing on diamond impregnated laps succeeded in producing surfaces which were flat to within $\pm \frac{1}{4}$ μ. The surface flatness, however, was achieved only at the expense of introducing large amounts of additional mechanical damage. Figure 1b shows the dislocation density to be increased by 2 orders of magnitude above the native dislocation density. Attempts to remove the damage by subsequent annealing at high temperatures were only partially successful. Anneals performed for 2 h at 1850° in argon, during which the specimen surface was loosely covered by a second crystal to prevent thermal

pitting, reduced the dislocation density by factors of only 2 to 3.

Chemical polishing with hot 85% phosphoric acid was used to remove the damage introduced by mechanical polishing. A number of procedures were explored in attempts to preserve surface flatness: hand lapping a crystal against a flat glass plate, or spinning the crystal in close proximity to a plate in an attempt to maintain laminar flow. Stationary crystals polished in either static or slowly agitated solutions gave results which were equally satisfactory. The kinetics of chemical polishing over a temperature range of 148° to 187°C were investigated in detail in order to establish optimum conditions for chemical polishing. The thickness of material removed varied linearly with time, and the rate of material removal is shown as a function of reciprocal temperature in Figure 2. These rates were increased by factors of 2 to 3 in slowly agitated solutions. At temperatures above 170°C, it was observed that pits rapidly developed. The most satisfactory polishes were obtained at 155°C when the sample was removed and rinsed with hot H_2O at 3 minute intervals to guard against possible formation of a deposit of reaction products. Figure 1c displays the microstructure of a crystal after nearly complete removal of the damaged layer. (It is of interest to note that the dislocations contained within subgrains appear to lie on (110) slip bands. This suggests that the native dislocation densities of the crystal may have originated through thermal stresses introduced during fabrication; both varieties of materials were prepared by arc-fusion processes). While mechanical damage could be successfully eliminated through chemical polishing, this was only achieved through compromise of the superior flatness of the mechanically polished surfaces.

Sample Fabrication Since MgO has an extremely high vapor pressure at elevated temperatures, it was necessary to inhibit volatilization of the

specimen surface and tracer isotope, and also to protect the sample from possible contamination derived from furnace elements during diffusion annealings. This was accomplished, as in a preceding study[7], by encapsulation of the entire diffusion specimen within a pressed cylinder of high-purity MgO powder. The polycrystalline compact sintered during the early portions of the diffusion annealing and entrapped the specimen.

Vapor-exchange specimens were employed at temperatures above 1600°C. Such specimens were prepared by ultrasonically machining a small well in a single crystal of the same material as that of the host crystal. The well was partially filled with $Mg^{26}O$. A prepared surface of the host crystal was placed over the well, and the assembly was then encapsulated. Because of the reduced vapor pressure of MgO at lower temperatures, this type of specimen could be employed only at temperatures above 1600°C.

Preparation of the thick-film specimens utilized at intermediate temperatures proved difficult. Ideally, the isotopic coating should be supplied as a dense layer in intimate contact with the host crystal. Attempts to produce such a coating through deposition of a slurry or, alternately, by spraying on a weakly acidic solution of the isotope proved unsuccessful. It was found that coatings applied by the latter method acquired impurity and, further, the films applied by both procedures peeled from the host crystal once a thickness of approximately 1 μ had been exceeded. The problem was successfully solved by application of chemical vapor transport procedures developed in this laboratory in an attempt to synthesize ultra-high purity MgO single crystals[26]. Using HCl as a transport agent, it was possible to grow a uniform layer of single crystal $Mg^{26}O$ epitaxially on the surface of the host crystal at a rate of 100 μ/h at 1000°C. All deposits applied were ca. 30 μ in thickness, so that the amount

of diffusion which occurred during deposition was negligible. Negligible concentrations ($<$10 ppm) of Cl were incorporated in the deposit. Not only was the requisite dense single-crystal layer of isotope applied to the host crystal, but it was demonstrated[26] that the transport process effected considerable purification of the isotope as well. For samples to be annealed at the lowest temperatures, a thickness of the epitaxial layer of isotope greater than the anticipated diffusion zone, was grown so that the semi-infinite source boundary conditions were valid.

All diffusion annealings were conducted in an argon atmosphere in electrical resistance furnaces controlled to $\pm$ 5°C. At temperatures of 1450°C and below, it proved unnecessary to encapsulate the specimens; not only was the vapor pressure of MgO greatly reduced, but the isotope-crystal interface was protected by an epitaxial layer which was thick compared with the extent of the anticipated diffusion zone. Upon completion of the diffusion annealings, at least 1 mm of material was trimmed from the sides of the specimens to eliminate the effects of surface diffusion.

Sample Analysis The trimmed diffusion specimens were mounted on the surface of a hardened steel cylinder which, in turn, rode snugly within a second concentric cylinder. The diffusion samples were sectioned by grinding with $\frac{1}{4}$ μ diamond paste on a sheet of Mo foil. The cylinder pair was supported by outriggers riding on an optical flat during this procedure. Surface roughness measurements indicated that parallelism and roughness of the surface could be maintained to within $\pm \frac{1}{4}$ μ. The thickness of the sections removed was determined through precision weighing after ultrasonic cleansing of the specimen. Areas of the trimmed specimens ranged from 0.5 to 1 cm^2, and sections down to 1.8 μ in thickness could be successfully removed and analyzed.

The isotopic composition of sections so removed was determined with the aid of mass spectrometry. Compared to the customary procedure of measurement of the activity of a radioisotope the present method had several advantages. Most importantly, the problems associated with the use of a short-lived radioisotope were avoided. The accuracy of a measurement was also not affected by accidental loss of a portion of a section inasmuch as an isotope ratio was determined. The principal disadvantage, on the other hand, was that the procedure was extremely time consuming. The system had to be baked out and evacuated upon introduction of each of the many sections obtained from each diffusion specimen. An additional disadvantage, peculiar to the system of the present study, was that the isotope concentrations had to be determined in the presence of a high background of natural abundance. The concentrations, unlike the situation of a radioisotope where the natural abundance is zero, were provided by the difference of two large numbers and were correspondingly less precise.

The bulk of the mass spectrometer analyses were conducted with a time-of-flight instrument. The grindings removed from the diffusion specimen were placed in a tungsten Knudsen effusion cell maintained at 1700°C. This produced a beam of Mg atoms which were directed into the ion source of the spectrometer. The beam was ionized by electron impact and mass analyzed. The spectral peaks at masses 24 and 26 were monitored simultaneously since the intensity of the beam was very sensitive to fluctuations in the temperature of the Knudsen cell. Measurement of the known natural abundance of Mg^{26} indicated that the isotopic composition of a 0.5 mg sample could be determined to within better than 1%.

Since the measurements were time consuming, a few supplemental analyses were performed with a double-focussing mass spectrometer which employed a

a triple-filament thermal-ionization source. In this technique the ratio of the mass peaks at 25 and 26 was obtained from photographic plates. Results comparable to those of the time-of-flight instrument were obtained and, through analysis of alternate sections of one diffusion sample with each of the two procedures, it was shown that results from the two instruments were indeed in complete accord.

RESULTS AND DISCUSSION

Typical concentration gradients for vapor-exchange specimens are presented in Fig. 3 where, according to (2), $\text{erfc}^{-1}\left[(C-C_0)/(C_S-C_0)\right]$ is plotted as a function of Mg^{26} penetration. Fig. 4 presents a concentration gradient obtained for the thick-film type of specimen prepared at intermediate temperatures. As mentioned above, the predicted distribution of solute for this type of specimen is such that the experimental result cannot be cast into a form in which a linear variation of a function of concentration with penetration yields a slope related to D. Also, the thickness of the layer of isotope could not be directly measured for this specimen because of the perfect epitaxy between host crystal and deposited isotope. (The thickness of the layer could not be determined by weight gain or direct measurement of sample thickness because the chemical vapor deposition procedure invariably resulted in removal of material from other surfaces of the specimen.) The gradient of Fig. 4 was analyzed in the following way. The gradient at large penetrations was fitted by (3) at large penetrations by least-squares techniques. The approximate fit to the data was used to obtain a preliminary value of 4Dt. The thickness of the isotopic layer, h, was then obtained in two ways: first by use of the value of 4Dt in (5), and, second, by integration of the isotopic content of the gradient and conversion of the value to an equivalent layer of pure isotope. The agreement of the estimates made in this fashion was remarkable: 10.77 μ in the former, and 10.81 μ in the latter. The computed value of h was then used in conjunction with the estimate of 4Dt to compute an exact solute distribution according to (4). It was intended to refine the value of 4Dt by iteration, but, as may be seen in Fig. 4, the degree of fit combined with the quality of the data did not justify any adjustment beyond the initial

estimate. The ambiguity involved in this type of specimen was seldom encountered because,at only slightly lower temperatures, the diffusion coefficients were sufficiently small that epitaxial layers of isotope large in comparison with the diffusion zone could be deposited without the need of sectioning through excessive thicknesses of material. Samples prepared at 1450°C and lower temperatures were prepared under conditions in which (6) was valid. Fig. 5 presents gradients in which $\text{erfc}^{-1}\left[2(C-C_0)/(C_s-C_0)\right]$ is plotted as a function of distance from the surface of the specimen. As has been noted, a value of h is not necessary for analysis of such data. Nevertheless, erfc^{-1} should be zero at the crystal-isotope interface. This was indeed the case. For the sample prepared at 1450°C, the thickness of the $Mg^{26}O$ layer was estimated to be $34.5 \pm 1.8\ \mu$, whereas erfc^{-1} was observed to be zero at $36.2 \pm 6.4\ \mu$; for the sample prepared at 1101°C, the corresponding values were $37.5 \pm 6.0\ \mu$ and $32.2 \pm 3.3\ \mu$.

Diffusion coefficients were obtained by fitting the expected solute distributions to the experimentally-measured gradients by least-squares techniques. Standard deviations in the diffusion coefficients so obtained ranged from 4.7 to 38.5% and averaged 14.1% for the entire set of measurements. (For gradients analyzed according to (2), of course, this represents twice the standard deviation of the least-squares fit to the slope of the actual gradient.) The higher standard deviations reflect a smaller number of data in shallow concentration gradients rather than poorer fit. Ten diffusion coefficients were obtained for Norton MgO, and three for Spicer MgO crystals over a temperature range of 1100° to 2400°C (0.45 to 0.87 T_m in °K). The diffusion coefficients and their standard deviations are summarized in Table III, and are plotted as a function of reciprocal temperature in Fig. 6. The data obtained for temperatures of 1450°C and above fit an

Arrhenius plot remarkably well, and a least-squares fit to the data obtained for the Norton crystals provides

$$D = 4.19 \, {}^{+2.45}_{-1.55} \times 10^{-4} \exp(-2.76 \pm .08 \text{ eV/kT})$$

The departure of the individual measurements from the Arrhenius plot range from 0.3 to 3.8 standard deviations and, for the entire set of data, average 1.18 σ. The diffusion coefficients obtained for the Spicer MgO crystals are included in Fig. 6. As in our earlier study of Ni^{2+} in these two materials[7], there is no significant difference in diffusion coefficients for the two materials. In the present work the difference between diffusion coefficients obtained for the two types of crystals is less than the sum of their standard deviations.

The diffusion coefficients obtained at 1257°C and 1101°C for the Norton crystals are as much as one order of magnitude too high relative to the remainder of the data. The reason for this departure will require further experimentation, but we believe that the effect is due to dislocation pipe diffusion. Very small diffusion coefficients were anticipated at these temperatures. The samples employed had therefore not received chemical polishing since it was felt that surface flatness was a stronger requisite than the absence of dislocations. These two crystals therefore possessed dislocation densities in the diffusion zone which were two orders of magnitude higher than in other specimens.

The diffusion coefficients obtained in the present study are much smaller than those reported by Lindner and Parfitt[2]. It therefore appears unlikely that the latter results represent intrinsic mass transport as had been previously supposed. The value of 10^{-4} for D_o, and the activation energy of 2.76 eV obtained in the present study are of magnitudes comparable to those obtained in measurements of impurity cation diffusion. We,

therefore, feel that the apparent anomaly in the cation self-diffusion data relative to the other transport data available for MgO has been resolved; the present data for Mg^{2+} self-diffusion, even at 2400°C and when employing the best crystals commercially available, also appears to represent extrinsic impurity-controlled diffusion. The present activation energy of 2.76 ± .08 eV is, in fact, remarkably close to the 2.6 eV energy of cation migration predicted for MgO on the basis of the empirical correlation with melting temperatures given by Barr and Dawson[23].

In recent months a second set of cation self-diffusion data, again obtained with the radioisotope Mg^{28} have been reported by Harding et al[27]. The data are also included in Fig. 6. As in the present work, two grades of crystals were employed. Those obtained from Monocrystals, Inc., Cleveland, Ohio, were found to contain ca. 540 ppm cation impurity, as obtained by emission spectrography, while material obtained from Ventron Electronics Corp., Bradford, Pennsylvania contain 450 ppm cation impurity. Below a temperature of 1300°C, both materials were considered to display equivalent transport behavior, and the data were described in terms of an activation energy of 3.2 eV. Lindner and Parfitt's data were assumed to represent intrinsic diffusion, and the 3.2 eV region was interpreted in terms of impurity precipitation ("Region IV", by convention). Above 1300°C, the data of Harding et al for the two grades of crystals appear to diverge. They described this region as representing extrinsic impurity-controlled diffusion being gradually influenced (on the basis of Lindner and Parfitt's data) by the onset of intrinsic behavior. They eventually infer an energy for Schottky pair formation of 3.4 ± .2 eV, and an energy for defect migration of 1.7 eV.

We prefer an alternative interpretation. The scatter in the data of Harding et al is such that the data for both materials may be represented almost equally well by a single Arrhenius fit over the entire temperature range of their investigation. A least-squares fit to all of the data obtained for the Monocrystals material provides

$$D = 7.81 \, {}^{+11.40}_{-\ 4.63} \quad 10^{-3} \quad \exp\,(-2.66 \pm .13 \text{ eV/kT}),$$

while a fit to the Ventron data provides

$$D = 1.84 \, {}^{+1.40}_{-0.80} \quad 10^{-3} \quad \exp\,(-2.51 \pm .08 \text{ eV/kT}).$$

If the data for both materials are combined

$$D = 3.62 \, {}^{+3.11}_{-1.67} \quad 10^{-3} \quad \exp\,(-2.58 \pm .09 \text{ eV/kT}).$$

The difference between the activation energy of the latter interpretation and the result of the present study is equal to the sum of the two standard deviations.

The order of magnitude difference in the magnitudes of the two investigations requires explanation. We would like to speculate on an interpretation which raises serious question concerning the validity of employing a short-lived radioisotope as a tracer in the study of diffusion in any ionic compound. What effect might the products of decay have when the result of transmutation is a cation of different valence? In particular, Mg^{28} decays, with a half-life of 21.3 h to Al^{28} which, in turn, decays to Si^{28} (stable) with a half-life of 2.3 min. The MgO host crystal is thus continually doped with an aliovalent impurity as a result of decay during the diffusion experiment. Mass transport under these conditions would be an extremely complex process since cation vacancies must be formed at a surface or internal boundary of the host crystal and diffuse to the Si ion formed by decay. At the very least, because of the short half-life of

Mg^{28}, one might conservatively estimate that at least 50% of an isotopic layer applied to a host crystal could conceivably consist of SiO_2. This could introduce significantly higher impurity contents than previously measured for a host crystal. The latter effect could be verified by a measurement in which a crystal was coated with a mixture of $Mg^{26}O$ and SiO_2. We plan to conduct such experiments. Regardless of the outcome, one should still question whether the impurities inherently introduced by the process of radioactive decay might prevent observation of intrinsic mass transport in crystals of any purity for ionic systems in which the only available radioisotope has a short half-life.

ACKNOWLEDGMENTS

The authorship of this paper only partially reflects the many individuals whose talents were brought to bear on this problem. The writers are pleased to acknowledge the contribution of W.H. Rhodes in performing the microstructure characterizations and the study of chemical polishing kinetics. P.E. Gruber developed the chemical vapor deposition procedures. We are also grateful for the assistance provided by A. Moschetti in the preparation of samples, F. Bourgelas in the time-of-flight spectrometer analyses, and K.S. Kim in the sectioning procedures. The spark-source chemical analyses and the triple-filament thermal-ionization determinations of isotope ratios were performed by D.C. Walters and E.R. Blosser of the Battelle Memorial Institute. The study was supported by the Advanced Research Projects Agency under Contract DAHC-15-68-C-0296.

REFERENCES

1. Y. Oishi and W.D. Kingery, J. Chem. Phys., 33, 905 (1960).
2. R. Lindner and G.D. Parfitt, J. Chem. Phys., 26, 182 (1957).
3. B.C. Harding and A.J. Mortlock, J. Chem. Phys., 45, 2699 (1966).
4. H. Tagai, S. Iwai, T. Iseki and M. Saho, Radex Rundschau, 4, 577 (1965).
5. M.F. Berard, J. Am. Ceram. Soc., 54, 58 (1971).
6. B.J. Wuensch and T. Vasilos, J. Chem. Phys., 36, 2917 (1962).
7. B.J. Wuensch and T. Vasilos, J. Chem. Phys., 54, 1123 (1971).
8. B.J. Wuensch and T. Vasilos, J. Chem. Phys., 42, 4113 (1965).
9. J. Rungis and A.J. Mortlock, Phil. Mag., 14, 821 (1966).
10. B.J. Wuensch and T. Vasilos, Nat'l. Bur. Std. (U.S.), Spec. Publ., 296, 95 (1968).
11. B.C. Harding, Phil. Mag., 16, 1039 (1967).
12. I. Zaplatynsky, J. Am. Ceram. Soc., 45, 28 (1962).
13. J.S. Choi, Ph.D. Thesis, Indiana University (1963).
14. S.L. Blank and J.A. Pask, J. Am. Ceram. Soc., 52, 699 (1969).
15. M. Appel and J.A. Pask, J. Am. Ceram. Soc., 54, 152 (1971).
16. E.B. Rigby and I.B. Cutler, J. Am. Ceram. Soc., 48, 95 (1965).
17. J.T. Jones and I.B. Cutler, J. Am. Ceram. Soc., 54, 335 (1971).
18. C. Greskovich and V.S. Stubican, J. Phys. Chem. Sol., 30, 909 (1969).
19. W.P. Whitney II and V.S. Stubican, J. Phys. Chem. Sol., 32, 305 (1971).
20. W.P. Whitney II and V.S. Stubican, J. Am. Ceram. Soc., 54, 349 (1971).
21. R.D. Shannon and C.T. Prewitt, Acta. Crystallogr., B25, 925 (1969).
22. J. Yamashita and T. Kurosawa, J. Phys. Soc. Japan, 9, 944 (1954).
23. L.W. Barr and D.K. Dawson, Proc. Brit. Ceram. Soc., 19, 151 (1971).
24. J.W. Cleland, Nat'l. Bur. Std. (U.S.), Spec. Publ., 296, 195 (1968).

25. J. Crank, The Mathematics of Diffusion, (Clarendon Press, Oxford, 1956), p. 13.

26. P.E. Gruber, "Growth of High Purity MgO Single Crystals by Chemical Vapor Transport Techniques," (to be submitted to J. Cryst. Growth).

27. B.C. Harding, D.M. Price, and A.J. Mortlock, Phil. Mag. 28, 399 (1971).

Table I Tracer-type diffusion data for MgO

Ion	Ionic radius[a] (10^{-8} cm)	Temperature range (°C)	D_0 (cm^2/sec)	E (eV)	Reference
Be^{2+}	0.27	1000-1700	$1.41\ 10^{-5}$	1.60	3
Cr^{3+}	0.615	1300-1700	$9.8\ 10^{-4}$	2.95	4
Ni^{2+}	0.700	1000-2460	$1.80\ 10^{-5}$	2.10	6,7
Mg^{2+}	0.720	1429-1616	$2.49\ 10^{-1}$	3.43	2
Co^{2+}	0.735	1000-1810	$5.78\ 10^{-5}$	2.06	6
Zn^{2+}	0.745	1000-1645	$1.48\ 10^{-5}$	1.85	8
Fe^{2+}	0.770	1050-1720	$8.93\ 10^{-5}$	1.81	6
		1310-1690	$3.2\ 10^{-4}$	1.82	4
Mn^{2+}	0.820	1300-1700	$4.1\ 10^{-7}$	1.21	4
Y^{3+}	0.892	1440-1760	$2.11\ 10^{-2}$	3.10	5
Ca^{2+}	1.00	910-1700	$2.95\ 10^{-5}$	2.13	9
		790-1850	$8.9\ 10^{-4}$	2.76	10
Ba^{2+}	1.36	1008-1724	$7\ 10^{-2}$	3.38[b]	11
			$6.3\ 10^{-5}$	1.85[c]	
O^{2-}	1.40	1300-1750	$2.5\ 10^{-6}$	2.71	1

[a] Ref. 21

[b] small solute penetrations

[c] large solute penetrations

Table II Spark-source mass spectrometer analysis of typical MgO crystals after utilization in diffusion couples (parts-per-million weight)

Element	Spicer MgO	Norton MgO	Element	Spicer MgO	Norton MgO
Li	0.06	0.2	Mn	2	20
Na	30	30	Fe	50	300
Al	20	30	Ni	3	7
Si	5	50	Cu	1	0.4
S	10	20	Zr	2	10
Cl	20	10	Ba	1	0.3
K	10	10	Pb	1	1
Ca	100	200	Bi	0.3	0.3
V	$\leq$ 2	$\leq$ 1	Σ cation	234	670
Cr	$\leq$ 4	7	Σ anion	30	30
			Total	264	700

Table III Cation self-diffusion coefficients in single-crystal MgO (uncertainty in D derived from standard deviation of least-squares fit to concentration gradient)

Temp (°C)	Time (h)	Specimen type[a]	D(cm^2/sec)	Analysis[b]
Norton MgO				
1101	2173.8	S	$2.81 \pm .21\ 10^{-13}$	K
1257	691.0	S	$1.74 \pm .13\ 10^{-12}$	K
1450	72.0	S	$3.67 \pm .50\ 10^{-12}$	K
1600	16.0	V	$1.38 \pm .44\ 10^{-11}$	K
1750	16.3	V	$5.71 \pm .51\ 10^{-11}$	K
1850[c]	15.7	V	$1.53 \pm .43\ 10^{-10}$	K
1950	8.0	V	$2.16 \pm .22$ 10-10	K
2050	6.0	V	$3.60 \pm .35\ 10^{-10}$	K,F
2250	5.0	V	$1.08 \pm .05\ 10^{-9}$	F
2400	2.0	V	$3.16 \pm .52\ 10^{-9}$	K
Spicer MgO				
1600	31.0	T	$1.95 \pm .06\ 10^{-11}$	F
1850[c]	15.7	V	$9.07 \pm 1.85\ 10^{-11}$	K
2400	2.0	V	$3.78 \pm .56\ 10^{-9}$	K

[a] V = vapor exchange
T = thick film
S = semi-infinite source

[b] K = Knudsen-cell source, time-of-flight spectrometer
F = triple-filament source, double-focusing spectrometer

[c] crystals used for analyses of Table II

FIGURE CAPTIONS

Fig. 1. Dislocations revealed by etch pits in MgO crystals subjected to various treatments. (a) Excess dislocations along (110) slip bands near cleavage step (running from upper left to lower right) on as-cleaved (100) surface of Spicer MgO crystal. Native dislocation density is visible at upper right. (b) Excess dislocations ($8.2\ 10^7\ cm^{-2}$) introduced by mechanical polishing of Norton MgO crystal cleavage surface to flatness of $\pm \frac{1}{4}\mu$. (c) Native dislocation density and subgrain structure revealed in Norton MgO single-crystal after removal of 40 μ of damaged material by chemical polishing in hot 85% orthophosphoric acid. A trace of the damage introduced by mechanical polishing is still visible.

Fig. 2. Kinetics of chemical polishing of MgO in hot 85% orthophosphoric acid. Rate of material removal as a function of reciprocal temperature. (Bars indicate extremes of dissolution rates observed.)

Fig. 3. Representative plots of the inverse complementary error function of normalized concentration as a function of penetration for vapor-exchange specimens. C_s is surface concentration of isotope expressed as atomic fraction $Mg^{26}O$; Co is natural abundance of $Mg^{26}O$. (2400°C gradient for Spicer MgO; remainder are Norton crystals. 2250° gradient based on Mg^{26}/Mg^{25} using triple-filament thermal-ionization spectrometer source; remaining data obtained from Mg^{26}/Mg^{24} using Knudsen-cell source).

Fig. 4. Concentration gradient obtained for a thick-film sample. Dashed curve is least-squares fit to high-penetration data of the Gaussian solute distribution valid for thin-film boundary

conditions. Solid curve gives exact solution based on the value of 4Dt so obtained. (Spicer MgO; gradient based on Mg^{26}/Mg^{25} using triple-filament thermal-ionization spectrometer source.)

Fig. 5. Representative plots of the inverse complementary error function of twice the normalized $Mg^{26}O$ solute concentration as a function of distance from the surface of the sample for semi-infinite source specimens (Norton MgO; gradients based on Mg^{26}/Mg^{24} using Knudsen cell spectrometer source).

Fig. 6 Cation self-diffusion coefficients in MgO as a function of reciprocal temperature.

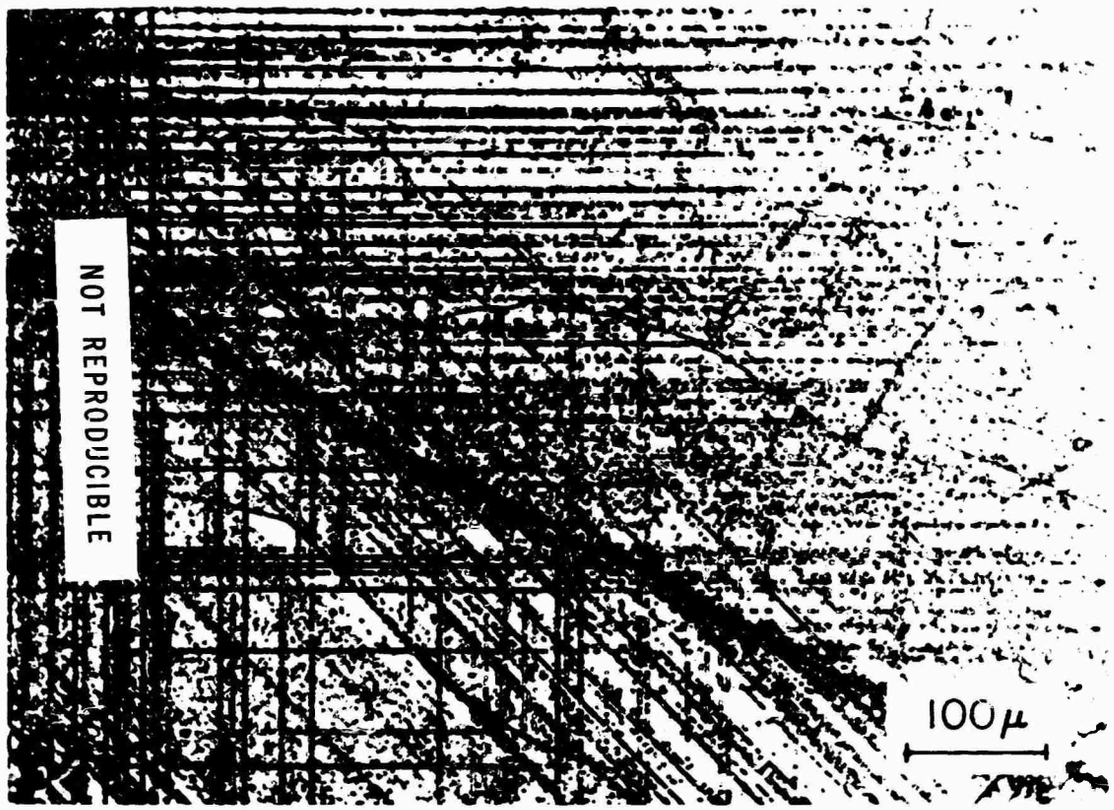

Figure 1a.

Excess dislocations along (110) slip bands near cleavage (100) surface of Spicer MgO crystal. Native dislocation density is visible at upper right.

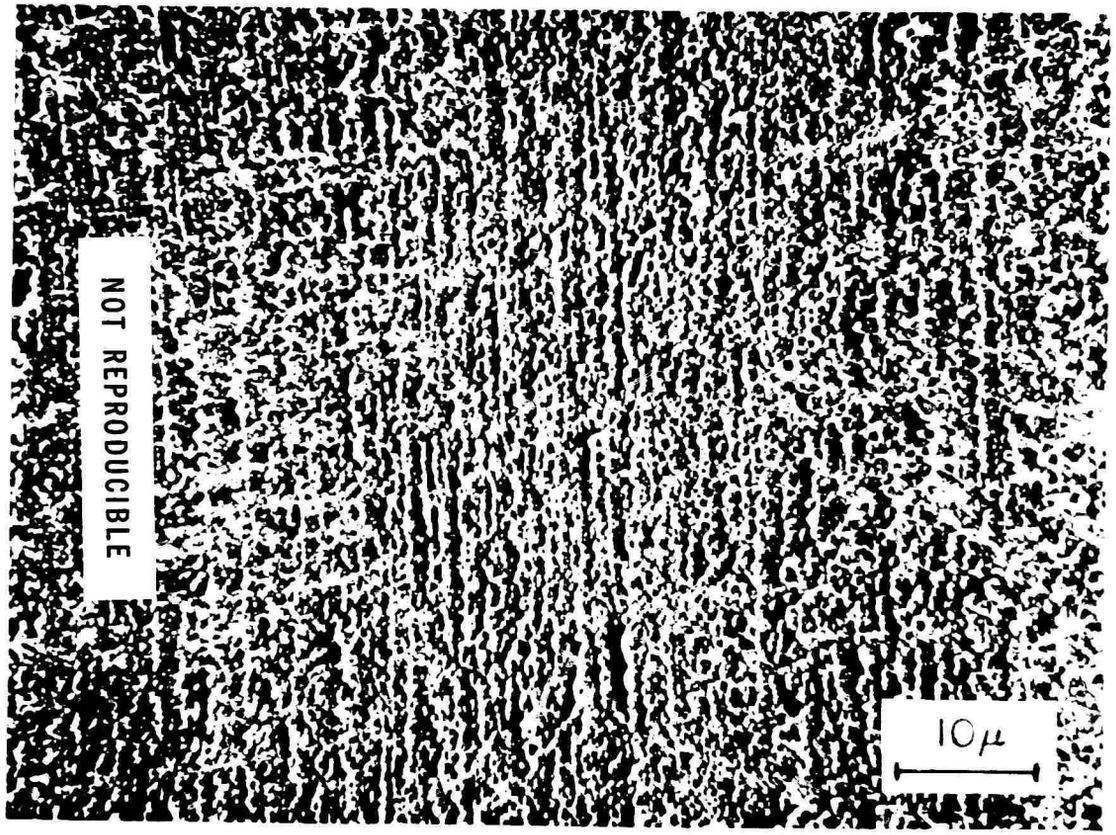

Figure 1b.

Excess dislocations ($8.2\ 10^{7}$ cm^{-2}) introduced by mechanical polishing of Norton MgO crystal cleavage surface to flatness of $\pm \frac{1}{4}\ \mu$.

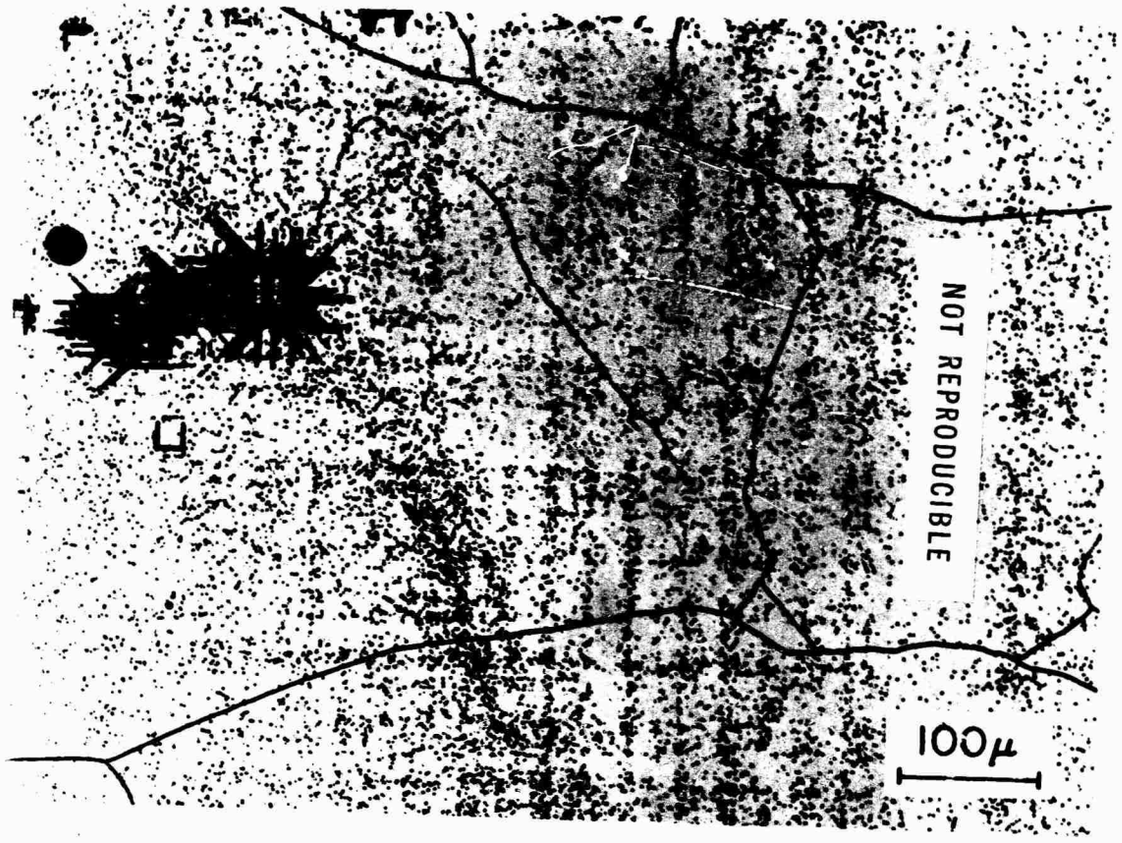

Figure 1c.

Native dislocation density and subgrain structure revealed in Norton MgO single crystal after removal of 40 u of damaged material by chemical polishing in hot 85% orthophosphoric acid. A trace of the damage introduced by mechanical polishing is still visible.

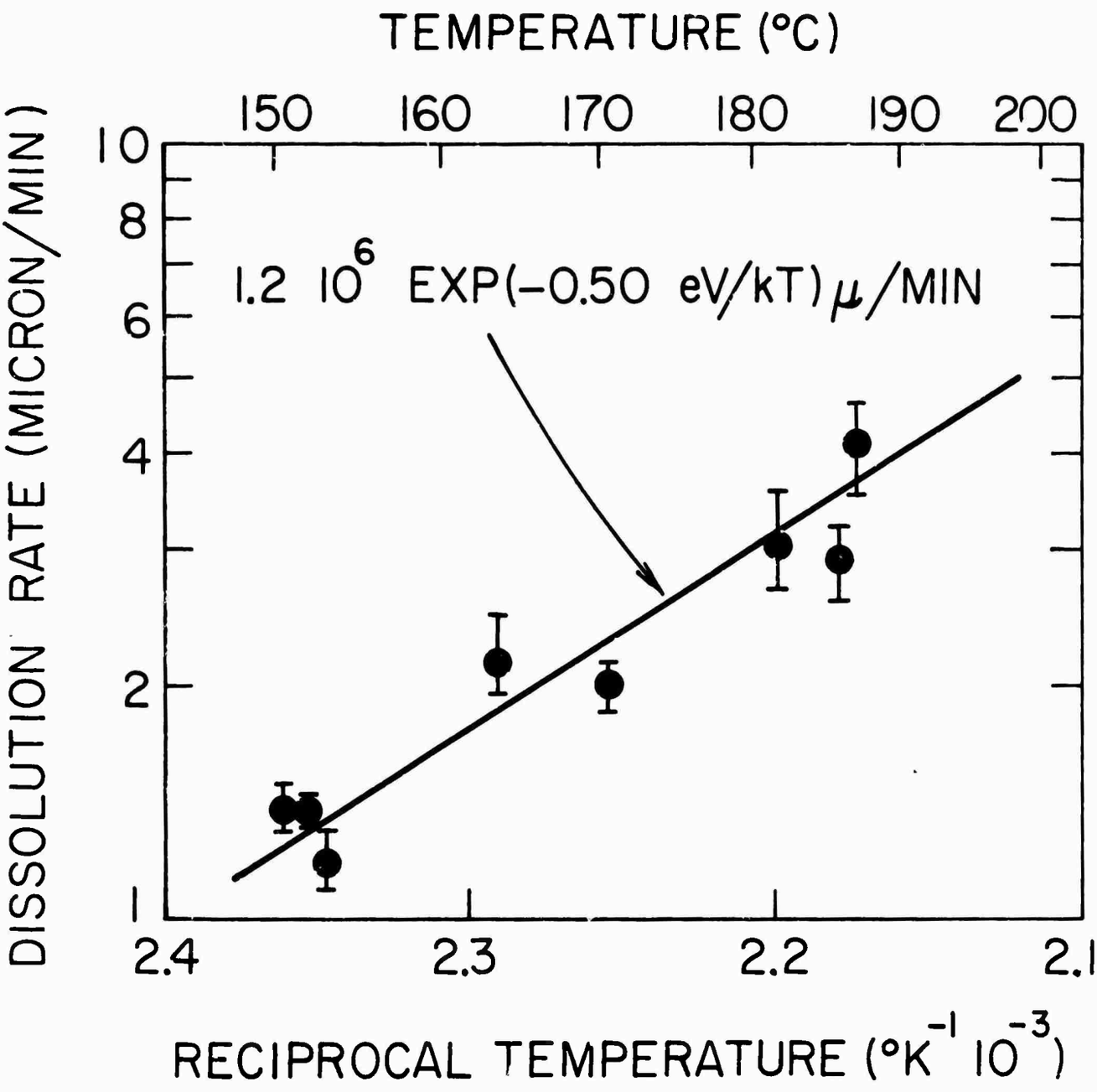

Figure 2.

Kinetics of chemical polishing of MgO in hot 85% orthophosphoric acid. Rate of material removal as a function of reciprocal temperature. (Bars indicate extremes of dissolution rates observed.)

55

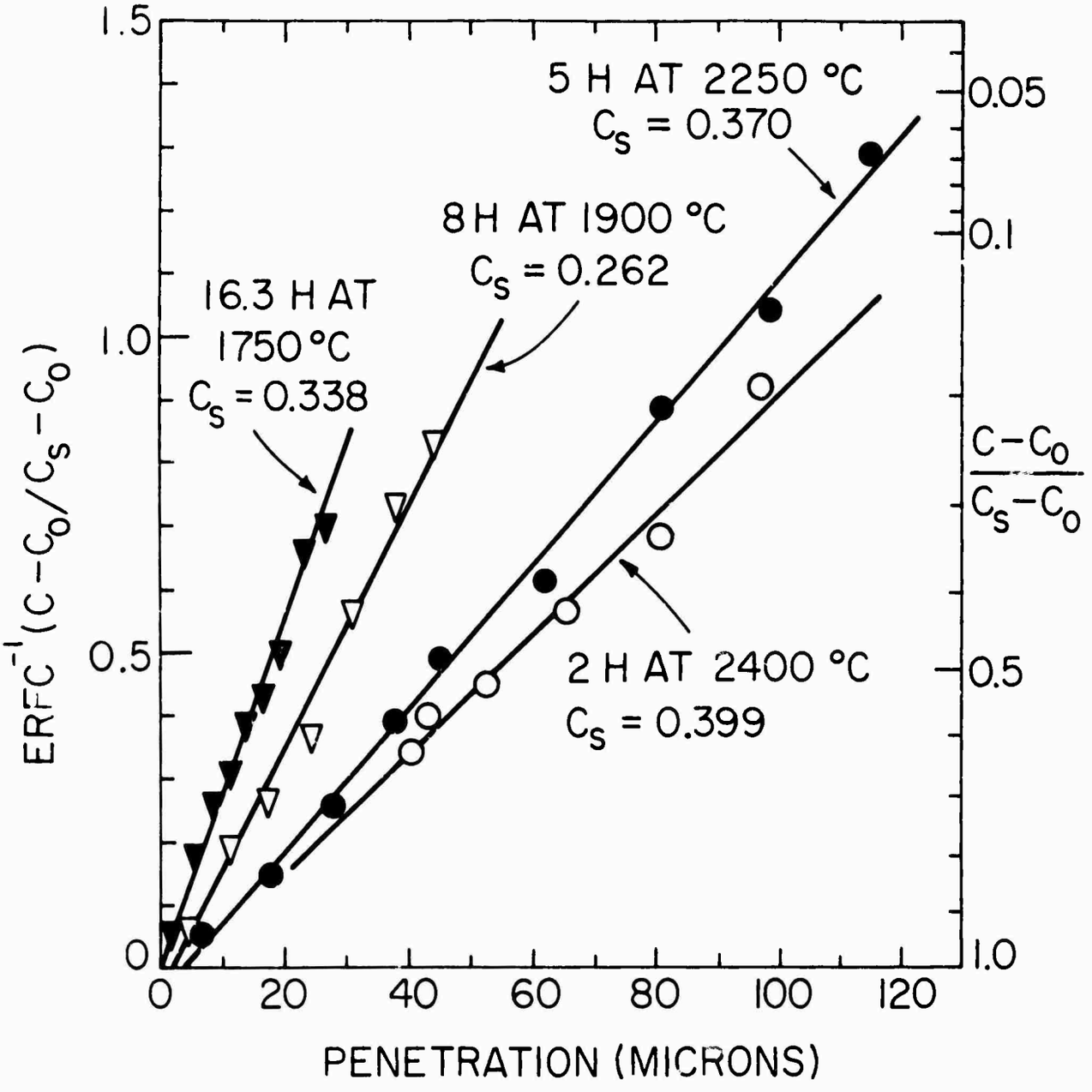

Figure 3.

Representative plots of the inverse complementary error function of normalized concentration as a function of penetration for vapor-exchange specimens. C_s is surface concentration of isotope expressed as atomic fraction Mg^{26}; Co is natural abundance of Mg^{26}. (2400°C gradient for Spicer MgO; remainder are Norton crystals. 2250° gradient based on Mg^{26}/Mg^{25} using triple-filament thermal-ionization spectrometer source; remaining data obtained from Mg^{26}/Mg^{24} using Knudsen-cell source.)

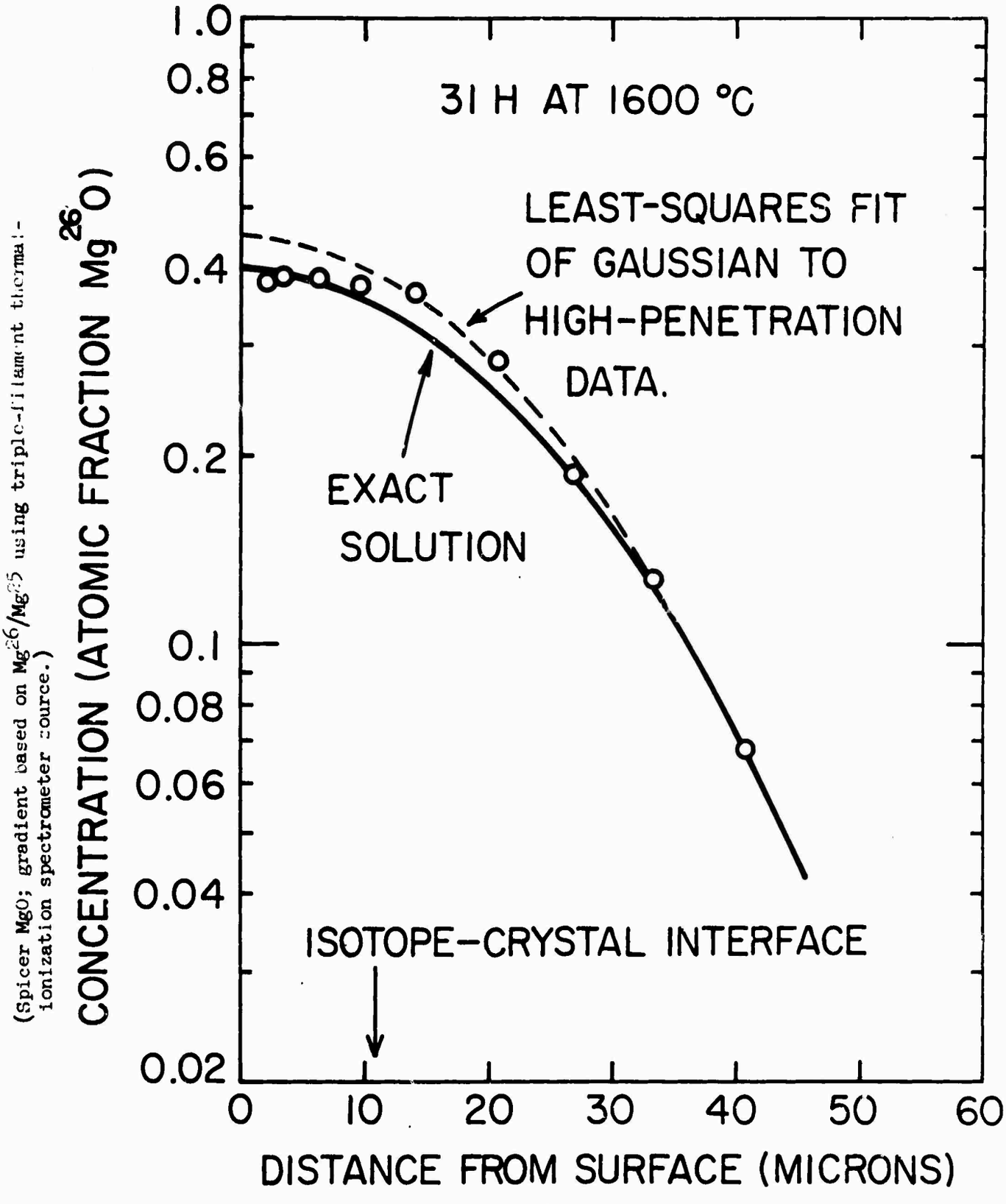

(Spicer MgO; gradient based on Mg^{26}/Mg^{25} using triple-filament thermal-ionization spectrometer source.)

Figure 4.

Concentration gradient obtained for a thick-film sample. Dashed curve is least-squares fit to high-penetration data of the Gaussian solute distribution valid for thin-film boundary conditions. Solid curve gives exact solution based on the value of 4Dt so obtained.

Figure 5. Representative plots of the inverse complementary error function of twice the normalized $Mg^{26}O$ solute concentration as a function of distance from the surface of the sample for semi-infinite source specimen. (Norton MgO; gradients based on Mg^{26}/Mg^{24} using Knudsen cell spectrometer source).

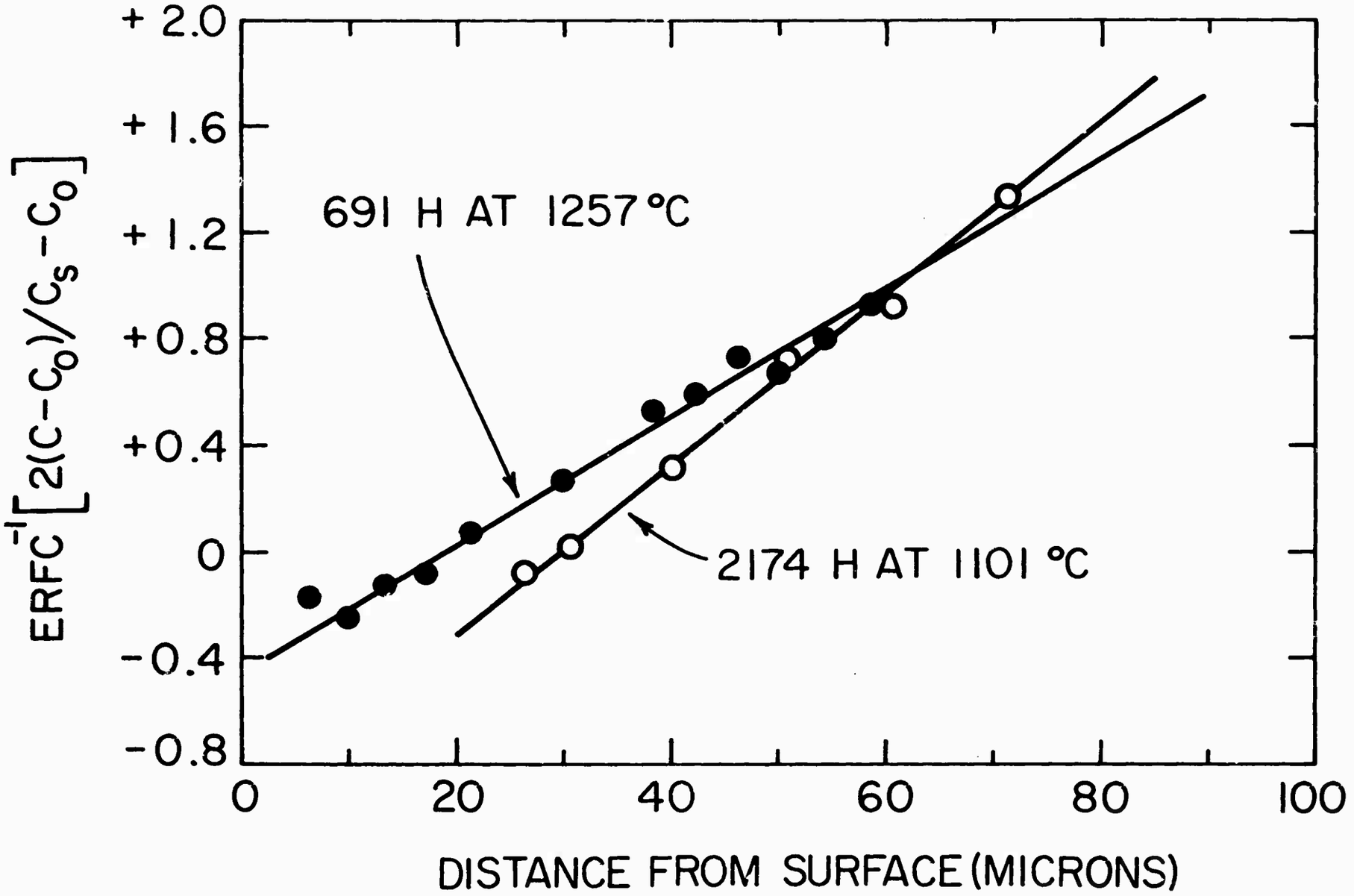

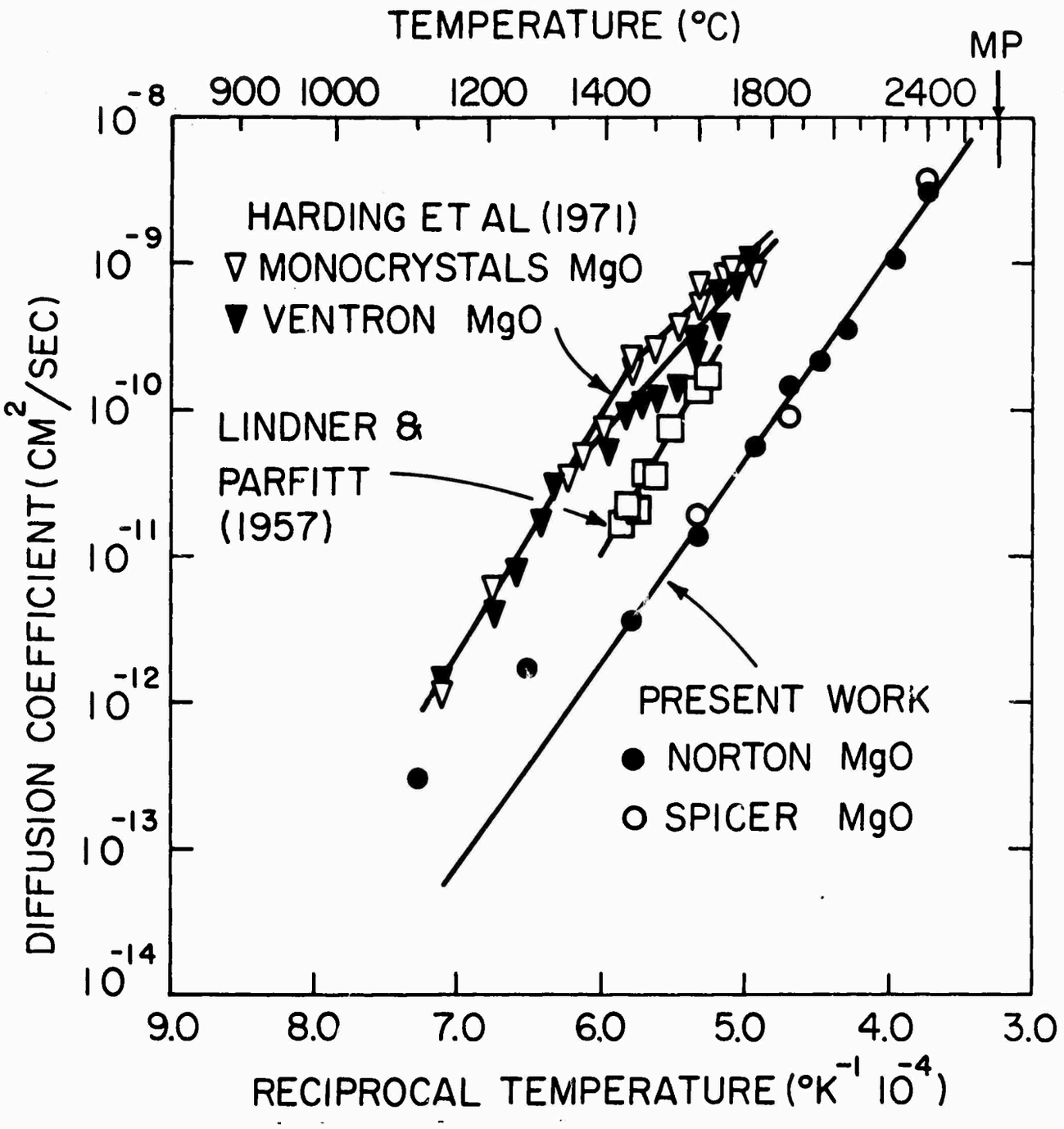

Figure 6.

Cation self-diffusion coefficients in MgO as a function of reciprocal temperature.

APPENDIX C

GROWTH OF HIGH PURITY MAGNESIUM OXIDE SINGLE CRYSTAL BY CHEMICAL VAPOR TRANSPORT TECHNIQUES

(Submitted to the Journal of Crystal Growth)

Growth of High Purity Magnesium Oxide Single Crystal by Chemical Vapor Transport Techniques

P.E. Gruber

Avco Corporation, Systems Division, Lowell, Massachusetts 01851

ABSTRACT

Single crystals of magnesia of very high purity and perfection, 21 mm x 1.5 mm were grown epitaxially by chemical vapor transport in HCl and H_2. Dislocation densities of 2×10^6 d/cm^2 were found in crystals grown on magnesia substrates having much higher dislocation densities.

INTRODUCTION

Single crystal magnesium oxide crystals have previously been made employing techniques of arc-fusion[1-5], flux[6,7], and chemical vapor deposition[8], but the method of chemical transport has received little attention since Sainte-Claire Deville's investigations[9] to explain the natural formation of mineral crystals. In the study described in this paper, MgO powder was transported in anhydrous HCl to the face of a MgO substrate crystal to form very pure epitaxial single crystal deposits. Experiments on the chemical transport of MgO in hydrogen also yielded single crystal deposits.

EXPERIMENTAL

The chemical transport of MgO[10] takes place in anhydrous HCl by virtue of the reversible reaction.

$$MgO + 2HCl \rightleftharpoons MgCl_2 + H_2O$$

in a thermal gradient maintained between the source MgO and the substrate crystal. Transport conditions and geometry were the subject of considerable experimentation in the evolution of the apparatus and procedure described below and in Figure 1. The pelletized source MgO powder was on the bottom of the platinum crucible and a ring of platinum foil supported the substrate crystal above the source. The crucible was closed with a snuggly fitting platinum foil cover and suspended in the qurtz chamber, as shown in Figure 1. The chamber was evacuated and the contents of the crucible baked-out at 1000°C for several hours, or until attaining a vacuum of approximately 10^{-6} torr. After allowing the crucible to cool, an amount of anhydrous HCl, corresponding to a pressure of 10-40 torr, was introduced into the chamber.

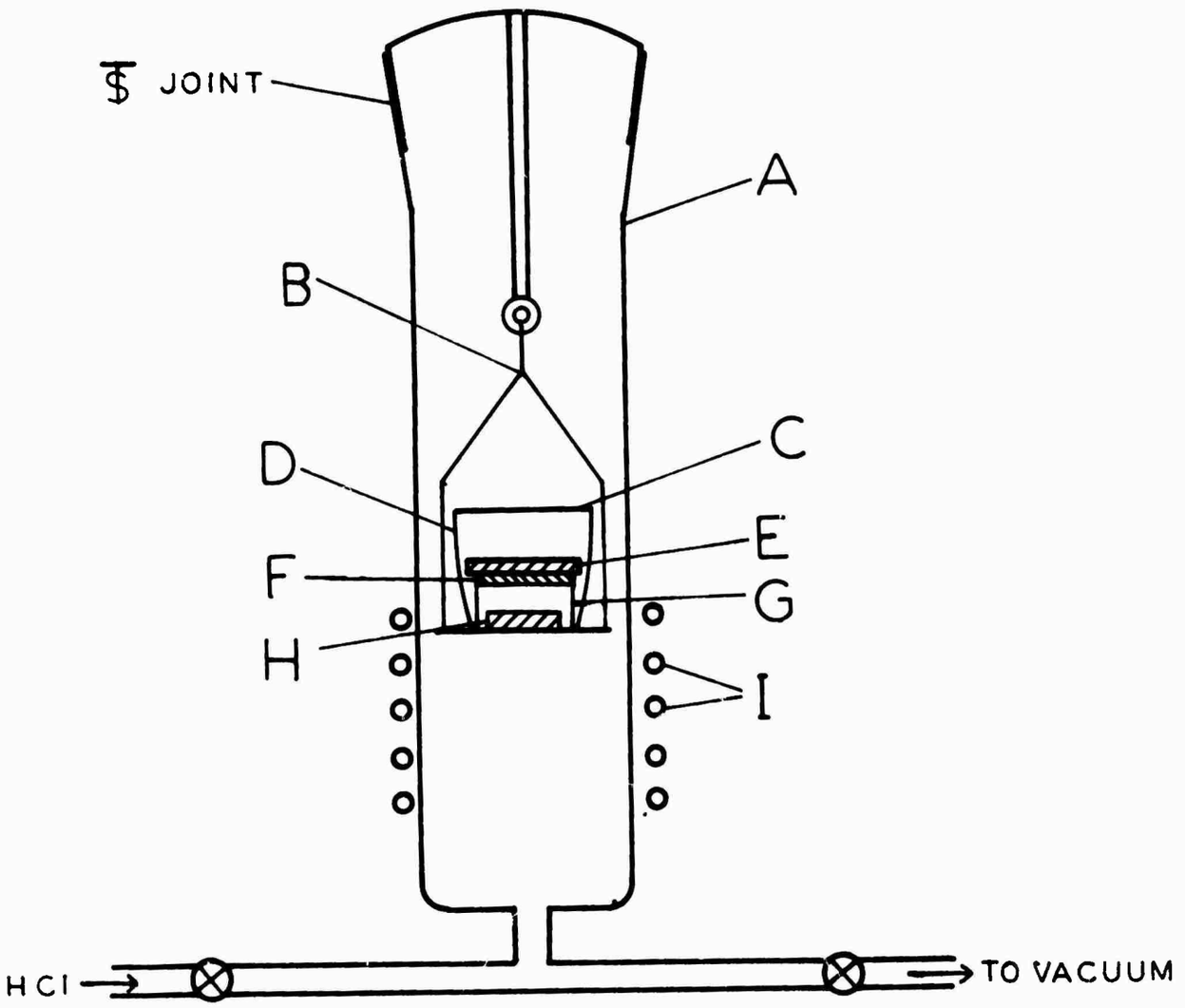

Figure 1.

Schematic of Apparatus for MgO Chemical Transport in HCl

A - Quartz Chamber
B - Pt Wire Support
C - Pt Foil Crucible Cover
D - Pt Crucible
E - Substrate Crystal
F - Growing MgO Deposit
G - Cylindrical Pt Seed Support
H - Pelletized Source MgO
I - RF Inductive Heating Coils

By proper positioning in the RF field, the platinum crucible was heated from the bottom, which provided the temperature gradient for chemical transport. In any given experiment, the crucible bottom temperature, as measured by an optical pyrometer, was held constant. Temperatures between 800°C and 1600°C were tried, but best results were obtained at 1000°C. The substrate, in almost all experiments, was the cleavage face (100) of a Norton MgO crystal. Both as-cleaved surfaces as well as surfaces chemically polished in hot phosphoric acid were used. In most experiments, the transport was allowed to proceed for about 12 hours. Experiments of longer duration encountered difficulty which resulted probably from the condensation of $MgCl_2$ and MgO on the inner walls of the quartz chamber; this loss of chloride to the chamber walls tended to retard the transport between the source MgO and the substrate. Wrapping the exterior of the chamber with heating tape was helpful when making experiments of longer duration.

The chemical transport of MgO in hydrogen was found to be possible, probably by the reaction

$$MgO + H_2 \rightleftharpoons Mg + H_2O$$

The hydrogen transport experiments were carried out in two cylindrical tungsten crucibles placed mouth-to-mouth, to form a closed transport system, in a hydrogen furnace. The crucibles were placed in the furnace such that a thermal gradient exacted between the source MgO in one crucible and the deposition area in the other crucible.

RESULTS AND DISCUSSION

Over 200 single crystal samples, many as large as 21 mm in diameter and some as thick as 1.5 mm, were made. Growth rates of approximately 100 μm/hour were routinely achieved in the later stages of this work. This rate compares very favorably with the best rates realized with other growth

techniques for MgO.

The chemical purity of two of the grown crystals, compared with two commercial crystals and the source MgO, was ascertained by complete spark source mass spectroscopic analysis (performed by Battelle Memorial Institute), presented in Table I. The two grown crystals are samples 175 and 180; the Norton[a] and the Spicer[b] crystals were vapor deposited at 1850°C. The source MgO for samples 175 and 180 was Johnson-Matthey[c] MgO powder.

The purity of crystals 175 and 180 is generally very much better than that of the Norton crystals. The comparison with Spicer crystals, however, shows Spicer to be slightly better. Three notable exceptions are Al, Ca, and Cl for which the grown crystals are better than the Spicer. The low concentration of Cl in these crystals is particularly significant, since contamination by the transporting agent, HCl, had been feared. Also gratifying is the fact that there is even considerably less Cl in these crystals than in source MgO.

The three impurities, Si, S, and Fe, are the greatest problem. Silicon may be preferentially transported from the source, although the possibility of contamination from the quartz reaction tube cannot be excluded. Some reduction in sulfur is realized in the transport of MgO, which indicates that this problem could be solved by ridding the source material of some of its sulfur (possibly present as sulfate residue remaining from the preparation of the source MgO). The worst offender is clearly Fe, which is apparently being preferentially transported from the source MgO. Iron contamination could possibly be reduced by pre-heating the source MgO in anhydrous HCl.

---

[a]Norton Co., Worcester, Massachusetts.

[b]W. & C. Spicer, Ltd., Winchcomb, Gloucestershire, England.

[c]Johnson-Matthey Chemicals, Ltd., London - Lot S-8573, obtained from United Mineral & Chemical Corp., New York City.

A problem which was encountered in many of the grown crystals was a slight brownish discoloration of the deposit. The conjecture that this discoloration might be due to platinum contamination was supported by the observation that in several cases in which the discoloration was particularly noticeable, small hexagonal platinum crystals were also observed around the periphery of the MgO deposit. Chemical transport of platinum in the HCl atmosphere could not be the cause of the discoloration, however, since the absence or amount of discoloration varied considerably in what were thought to be duplicate experiments. Further observations led to the hypothesis that the appearance of the discoloration was related to small air leaks into the partial vacuum inside the quartz chamber. This was confirmed in an experiment in which an amount of air corresponding to a pressure of 10 torr was introduced along with 40 torr of HCl. The resulting deposit, crystal 175, was nearly black and the chemical analysis of this sample was virtually the same (Table I) as that of a colorless one (180) except for the presence of 1000 ppm of platinum. The chemical transport of platinum has been observed in oxygen[11,12]. The discoloration is thus ascribed to platinum impurity in the MgO deposit, brought about by the transport of platinum in a trace of oxygen which occasionally leaked into the chamber.

Microscopic examination of a cleavage face through the substrate and the grown crystal, perpendicular to the growth direction, shows numerous cleavage steps running from the substrate across the interface into the deposit. This indicates that the deposited crystal was a structural continuation of the substrate crystal. Further evidence of the epitaxial nature of the deposit was given by von Laue reflection pattern of a 500 μm thick deposit on its substrate, which showed only one orientation and one crystal pattern.

TABLE I

Mass Spectrographic Analysis of MgO Crystals and Source Powder (ppmw)

Element	Sample Designation 175	180	Source MgO S8573	Norton Crystal	Spicer Crystal
Li	0.06	< 0.002	0.6	0.2	0.06
B	(a)	(a)	0.6	(a)	(a)
F	< 5.	< 5.	< 5.	< 5.	< 5.
Na	30.	60.	60.	30.	30.
Al	20.	10.	3.	30.	20.
Si	100.	50.	5.	50.	5.
P	2.	1.	< 1.	< 1.	< 1.
S	50.	50.	200.	20.	10.
Cl	10.	10.	20.	10.	20.
K	20.	20.	10.	10.	10.
Ca	≦ 30.	≦ 30.	≦ 30.	200.	100.
Sc	< 0.1	< 0.1	< 0.1	< 0.1	< 0.3
Ti	< 5.	< 2.	< 5.	< 5.	< 5.
V	≦ 0.5	≦ 0.5	≦ 0.5	≦ 1.	≦ 2.
Cr	< 1.	< 1.	< 1.	7.	≦ 4.
Mn	5.	0.7	5.	20.	2.
Fe	150.	150.	30.	300.	50.
Co	≦ 0.4	≦ 0.4	≦ 0.4	≦ 0.4	≦ 0.4
Ni	7.	3.	7.	7.	3.
Cu	1.	0.4	1.	0.4	1.
Zn	≦ 2.	≦ 2.	≦ 2.	≦ 1.	≦ 2.
Ga	< 0.4	< 0.4	< 0.4	< 0.1	< 0.1
Ge	≦ 1.	≦ 1.	≦ 1.	< 0.4	< 0.4
As	< 0.2	< 0.2	< 0.2	< 0.2	< 0.2
Se	< 1.	< 1.	< 1.	< 1.	< 1.
Br	1.	≦ 1.	≦ 1.	≦ 1.	≦ 1.
Rb	1.	< 0.2	< 0.2	< 0.2	< 0.2
Sr	< 0.2	< 0.2	< 0.2	< 0.2	< 0.2
Y	< 0.2	< 0.2	< 0.2	< 0.2	< 0.2
Zr	6.	2.	≦ 0.5	10.	2.
Nb	< 0.2	< 0.2	< 0.2	< 0.2	< 0.2
Mo	< 1.	< 1.	< 1.	< 1.	< 1.
Ru	< 0.3	< 0.3	< 0.3	< 0.3	< 0.3
Rh	3.	< 0.1	< 0.1	< 0.1	< 0.1
Pd	< 1.	< 1.	< 1.	< 1.	< 1.
Ag	< 2.	< 2.	< 2.	< 2.	< 2.
Cd	< 1.	< 1.	< 0.3	< 0.3	< 0.3
In	< 0.3	< 0.3	< 0.3	< 0.1	< 0.1
Sn	≦ 1.	≦ 1.	≦ 1.	< 1.	< 0.3
Sb	< 0.2	< 0.2	< 0.2	< 0.2	< 0.2
Te	< 1.	< 1.	< 1.	< 1.	< 1.
I	< 1.	< 1.	< 1.	< 1.	< 1.
Cs	< 0.1	< 0.1	< 0.1	< 0.1	< 0.1

TABLE I cont.

Element	Sample Designation 175	180	Source MgO S8573	Norton Crystal	Spicer Crystal
Ba	0.3	0.3	0.6	< 0.3	< 1.
La	≤ 4.	≤ 4.	≤ 4.	< 0.1	< 0.1
Ce	≤ 2.	≤ 2.	≤ 1.	< 0.1	< 0.1
Pr	< 0.1	< 0.1	< 0.1	< 0.1	< 0.1
Nd	< 0.4	< 0.4	< 0.4	< 0.4	< 0.4
Sm	< 0.4	< 0.4	< 0.4	< 0.4	< 0.4
Eu	< 0.2	< 0.2	< 0.2	< 0.2	< 0.2
Gd	< 0.4	< 0.4	< 0.4	< 0.4	< 0.4
Tb	< 0.1	< 0.1	< 0.1	< 0.1	< 0.1
Dy	< 0.4	< 0.4	< 0.4	< 0.4	< 0.4
Ho	< 0.1	< 0.1	< 0.1	< 0.1	< 0.1
Er	< 0.3	< 0.3	< 0.3	< 0.3	< 0.3
Tm	< 0.3	< 0.3	< 0.3	< 0.3	< 0.3
Yb	≤ 5.	≤ 5.	≤ 5.	< 0.5	< 0.5
Lu	< 0.1	< 0.1	< 0.1	< 0.1	< 0.1
Hg	< 200.(b)	< 200.(b)	< 0.5	< 50.(b)	< 50.(b)
Ta	< 15.(b)	< 15.(b)	≤ 2.	< 15.(b)	< 15.(b)
W	< 50.(b)	< 20.(b)	< 0.5	< 20.(b)	< 20.(b)
Re	< 0.3	< 1.	< 0.3	< 0.3	< 0.3
Os	< 0.4	< 1.	< 0.4	< 0.4	< 0.4
Ir	< 0.2	< 1.	< 0.3	< 0.3	< 0.3
Pt	1000.(c)	< 2.	4.	< 0.5	< 0.5
Au	< 0.5	< 0.5	< 0.5	< 0.5	< 0.5
Hg	< 0.5	< 2.	< 0.5	< 0.5	< 0.5
Tl	< 0.2	< 0.2	< 0.2	< 0.2	< 0.2
Pb	2.	2.	6.	1.	1.
Bi	0.6	0.6	0.6	0.3	0.3
Th	< 0.2	< 0.6	< 0.2	< 0.2	< 0.2
U	< 0.2	< 0.6	< 0.2	< 0.2	< 0.2

(a) Samples crushed in boron carbide mortar.

(b) Mortar contamination.

(c) Intentional Pt contamination.

Dislocation densities were determined by the etch pit technique using an etchant consisting of 5 parts saturated NH_4Cl, 1 part conc. H_2SO_4, and 1 part distilled water. The dislocation density on the surface of several as-grown crystals was found to be approximately 2×10^6 d/cm^2, 1 to 2 orders of magnitude less than found in the substrate crystals. The fate of some dislocations can be seen in Figure 2 which shows a cleaned and etched cross-section through the substrate and deposit of sample 96. Figure 2a shows two sites on the surface of the substrate where cleavage-induced slip on (110) caused dislocations in the adjacent deposit. As growth progressed, however, these dislocations gradually disappeared. Similarly, dislocations in the deposit, induced by the dislocations at the subgrain boundary shown in Figure 2b, also disappear. This suggests that thicker deposits might have still lower dislocation densities.

In preparing higher quality crystals, the cleavage damage present in the substrate of sample 96 was just removed by etching approximately 40 μm from the surface of the substrate with hot phosphoric acid.

Single crystals of MgO were also grown by chemical transport in H_2. With the source MgO powder at 1800°C and the substrate at 1750°C, many separate crystals, about 1 mm cubes, grew in 8 hours on the interior of the crucible near but not on the substrate crystal.

Chemical analyses for 10 possible impurities were performed by emission spectrography on one of the hydrogen grown crystals and on the source powder, (Fischer electronic grade). The analyses were semi-quantitative in that comparison was made with standards sparked at 10, 100, and 1000 ppm levels with no attempt to interpolate between these impurity levels. The results, presented in Table II, indicate purification with respect to Fe and Mn, but

Pl 5537-2 (a)

NOT REPRODUCIBLE

Pl 5537-3 (b)

Figure 2. Photomicrographs of Sample Cross-Section Showing Etch Pits

an enrichment in Al and Cr occurred in the transport and growth process. It is conjectured that these purifications and enrichments result from chemical transport reactions of these impurities, analogous to (but kinetically different) the transport of MgO.

It might be argued that simple thermal vaporization of MgO rather than chemical transport in H_2, could account for the growth of these crystals. The evidence, however, would indicate that chemical transport is the more likely mechanism. Porter[14] found that thermal vaporization of MgO is accompanied by dissociation. At 1950°K, approximately the temperature at which these crystals were grown, he found the partial pressure of Mg to be less than 5.7×10^{-5} torr. The equilibrium partial pressure of Mg over MgO in hydrogen, computed from thermochemical data[15], is 8×10^{-2} torr. The chemical transport of MgO in hydrogen would, therefore, appear to be more likely than thermal transport.

TABLE II

Impurities in Hydrogen Transported MgO Crystals

Element	Semi-quantitative Impurity Level (ppm) Grown Crystal	Source Powder
B	<100	<100
Al	1000	>100
Si	>1000	>1000
Ca	>1000	>1000
Ti	< 10	< 10
Cn	> 100	Not Detected
Mn	< 10	> 100
Fe	< 100	100
Cu	> 10	> 10
Zn	Not Detected	Not Detected

CONCLUSION

Single crystals of MgO having a very high degree of purity and perfection can be made by chemical transport in HCl. A reduction of some impurities in the source MgO powder is inherent in the transport. Crystals of still greater purification might be realized by further purification of the starting material.

REFERENCES

1. C.T. Butler, B.J. Sturm, and R.B. Quincy, J. Cryst. Growth, 8, 197 (1971).
2. L.J. Schupp, Electrochemical Technology 1968, 6 (5-6), 219-21
3. S.G. Tresvyatskii; V. Ya. Karpenko, V.L. Gol'Dshtein, Isobret., Prom. Obraztsy, Tovarnye, Znaki 1967, 44 (13), 21 U.S.S.R., 197, 525 (1967).
4. J.J. Scott, and N.C. Turnbull, U.S. 3, 245, 761 (1966).
5. A.E. Gorum, E.R. Parker and J.A. Pask, J. Am. Ceram. Soc., 41, 161 (1958).
6. H. Vora and R.R. Zupp, Mat. Res. Bull., 5, 977-982 (1970).
7. F.W. Webster, E.A.D. White, J. Crystal Growth, 5, 167-170 (1970).
8. J.E. Mee and G.R. Pulliam, International Conference on Crystal Growth, Boston, 1966; H. Steffen Peiser, Ed., Pergamon Press, Oxford,(1967).
9. H. Sainte-Claire Deville, Ann. 120, 176 (1861), Compt. rend. acad. sci. 52, 1264 (1861), ibid 53, 161 (1861).
10. H. Schäfer, "Chemical Transport Reactions," Academic Press, New York (1964), translated from "Chemishe Transportreaktionen", Verlag Chemie, Weinheim/Bergstr. (1962).
11. H. Schäfer and A. Tebben, Z. Anorg. Allgem. Chem. 304, 317 (1960).
12. G.W. Hooper and P. Hautefeuille, Compt. Rend. Acad. Sci. 84, 946 (1877).
13. R.J. Stokes, T.L. Johnson, and C.H. Li, Phil. Mag. 3, 718 (1958).
14. B.F. Porter, W.A. Chupka, and M.G. Inghram, J. Chem. Phys., 23, 1347 (1955).
15. O. Kubaschewski and E.L.L. Evans, "Metallurgical Thermochemistry," J. Wiley & Sons, New York, 1956, 227.

ACKNOWLEDGMENTS

The author is indebted to the Advanced Research Projects Agency for its support of this work under Contract DAHC 15-68-C-0296. The active interest and encouragement of Dr. A.D. Franklin throughout the program was greatly appreciated. Special thanks go to Drs. B.J. Wuensch and T. Vasilos for their inspiration and many fruitful discussions. The valuable assistance rendered by Dr. W.H. Rhodes in measuring dislocation densities, P. Berneburg in performing X-ray analyses, R.E. Gardner in metallographic preparation, and F. Kochanek, S. Basta, and T. Moschetti in performing crystal growth experiments, are gratefully acknowledged.